Journal of Visualized Experiments
Quantitative analysis of cell edge dynamics during cell spreading
--Manuscript Draft--

Article Type:	Methods Article - Author Produced Video
Manuscript Number:	JoVE62369R1
Full Title:	Quantitative analysis of cell edge dynamics during cell spreading
Corresponding Author:	Sergey V Plotnikov, PhD University of Toronto Toronto, Ontario CANADA
Corresponding Author's Institution:	University of Toronto
Corresponding Author E-Mail:	sergey.plotnikov@utoronto.ca
Order of Authors:	Ernest Iu
	Alexander Bogatch
	Sergey V Plotnikov, PhD
Additional Information:	
Question	**Response**
Please indicate whether this article will be Standard Access or Open Access.	Standard Access (US$1200)
Please specify the section of the submitted manuscript.	Biology
Please confirm that you have read and agree to the terms and conditions of the author license agreement that applies below:	I agree to the Author License Agreement
Please provide any comments to the journal here.	
Please indicate whether this article will be Standard Access or Open Access.	Standard Access ($1400)

1   **TITLE:**
2   Quantitative Analysis of Cell Edge Dynamics During Cell Spreading
3
4   **AUTHORS AND AFFILIATIONS:**
5   Ernest Iu[1,*], Alexander Bogatch[1,*], Sergey V Plotnikov[1]
6
7   [1]Department of Cell and Systems Biology, University of Toronto, Ontario, Canada
8
9   *These authors contributed equally.
10
11 Email addresses of co-authors:
12 Ernest Iu   (ernest.iu@mail.utoronto.ca)
13 Alexander Bogatch   (alexander.bogatch@mail.utoronto.ca)
14
15 Corresponding author:
16 Sergey V Plotnikov   (sergey.plotnikov@utoronto.ca)
17

18 **SUMMARY:**
19 In this protocol, we present the experimental procedures of a cell spreading assay that is based
20 on live-cell microscopy. We provide an open-source computational tool for the unbiased
21 segmentation of fluorescently labeled cells and quantitative analysis of lamellipodia dynamics
22 during cell spreading.
23

24 **ABSTRACT:**
25 Cell spreading is a dynamic process in which a cell suspended in media attaches to a substrate
26 and flattens itself from a rounded to a thin and spread-out shape. Following the cell-substrate
27 attachment, the cell forms a thin sheet of lamellipodia emanating from the cell body. In the
28 lamellipodia, globular actin (G-actin) monomers polymerize into a dense filamentous actin (F-
29 actin) meshwork that pushes against the plasma membrane, thereby providing the mechanical
30 forces required for the cell to spread. Notably, the molecular players that control the actin
31 polymerization in lamellipodia are essential for many other cellular processes, such as cell
32 migration and endocytosis.
33

34 Since spreading cells form continuous lamellipodia that span the entire cell periphery and
35 persistently expand outward, cell spreading assays have become an efficient tool to assess the
36 kinetics of lamellipodial protrusions. Although several technical implementations of the cell
37 spreading assay have been developed, a detailed description of the workflow, which would
38 include both a step-by-step protocol and computational tools for data analysis, is currently
39 lacking. Here, we describe the experimental procedures of the cell spreading assay and present
40 an open-source tool for quantitative and unbiased analysis of cell edge dynamics during
41 spreading. When combined with pharmacological manipulations and/or gene-silencing
42 techniques, this protocol is amenable to a large-scale screen of molecular players regulating
43 lamellipodial protrusions.
44

INTRODUCTION:

Lamellipodial protrusions are prominent membrane structures formed at the front of a migrating cell. In lamellipodia, polymerization of actin with the aid of the Arp2/3 complex and formins[1, 2] creates a fast-growing branched actin meshwork that pushes against the plasma membrane. The pushing force generated by the actin meshwork physically propels the cell forward[1, 3–5]. Depletion of the Arp2/3 complex or disruption of signaling pathways essential for lamellipodial protrusions often impair cell migration[6, 7]. Although migration of lamellipodia-deficient cells has also been reported[8, 9], the importance of lamellipodia in cell migration is evident as depletion of this protrusive structure perturbs the cell's ability to move through a complex biological microenvironment[6, 10].

A major hindrance to understanding the regulation of lamellipodia in migrating cells is the natural variability in lamellipodial protrusion kinetics, size, and shape[11–14]. Furthermore, recent studies have demonstrated that lamellipodia exhibit complex protrusive behaviors, including fluctuating, periodic, and accelerating protrusions[14, 15]. Compared to the highly variable lamellipodia of migrating cells[6, 16], lamellipodia formed during cell spreading are more uniform[12]. Since the protrusive activity of spreading and migrating cells is driven by identical macromolecular assemblies, which include a branched actin network, contractile actomyosin bundles, and integrin-based cell-matrix adhesions[17, 18], spreading cells have been widely used as a model for investigating the regulation of lamellipodia dynamics.

Cell spreading is a dynamic mechanochemical process where a cell in suspension first adheres to a substrate through integrin-based adhesions[17, 19, 20] and then spreads by extending actin-based protrusions[21–23]. During the spreading phase, lamellipodia emanating from the cell body protrude isotropically and persistently with little to no retraction or stalling[12]. The most commonly used cell spreading protocols are endpoints assays, where spreading cells are fixed at various times after plating[19, 24]. These assays, although quick and simple, are limited in their diagnostic power to detect changes in the dynamic features of lamellipodia. To determine the molecular mechanisms that control lamellipodia dynamics, the Sheetz group pioneered the use of quantitative analysis of live spreading cells and uncovered many fundamental properties of cell edge protrusions[11, 12, 22]. These studies have demonstrated that the live-cell spreading assay is a robust and powerful technique in the toolbox of a cell biology laboratory. Despite that, a detailed protocol and open-source computational tool for a live-cell spreading assay are currently unavailable for the cell biology community. To this end, our protocol outlines the procedures of imaging live spreading cells and provides an automated image analysis tool. To validate this method, we used Arp2/3 inhibition as an experimental treatment and showed that inhibiting the function of the Arp2/3 complex did not arrest cell spreading but caused a significant reduction in cell protrusion speed, as well as the stability of cell edge protrusions, giving rise to jagged cell edges. These data demonstrate that the combination of live-cell imaging and automated image analysis is a useful tool for analyzing cell edge dynamics and identifying molecular components that regulate lamellipodia.

PROTOCOL:

89   **1.   Cell Seeding**

90

91   NOTE: The described cell spreading protocol was performed using mouse embryonic fibroblasts
92   (MEFs) expressing PH-Akt-GFP (a fluorescent marker for $PIP_3/PI(3,4)P_2$). This cell line was
93   generated by genomically integrating an expression construct for PH-Akt-GFP (Addgene #21218)
94   by CRISPR-mediated gene editing. However, other fluorescent markers that are expressed
95   transiently or integrated in the genome can also be used in this assay. For optimal image
96   segmentation, we recommend using fluorescent markers that are evenly distributed in the
97   cytoplasm, *e.g.,* cytosolic GFP.

98

99   1.1   Culture a 10 cm dish of cells to 90% confluency.

100

101   1.2   Once the cells have attained the proper confluency, place a 22 mm x 22 mm coverslip
102   (#1.5; 0.17 mm thickness) into a 35 mm cell culture dish. Coat the coverslip with 400 μL of
103   fibronectin that has been diluted in PBS to a final concentration of 2.5 μg/mL.

104

105   NOTE: The number of coverslips required for the assay is determined by the number of
106   experimental conditions and technical replica.

107

108   1.3   Place the 35 mm dish with the fibronectin-coated coverslip into a 37 °C, 5% CO_2 incubator
109   for 1 hour.

110

111   1.4   Remove the dish with the coverslip from the incubator. Aspirate the fibronectin and wash
112   the coverslip with PBS by gently pipetting around the coverslip two to three times.

113

114   1.5   Aspirate the cell culture media from the 10 cm dish of cells and wash the dish with PBS.

115

116   1.6   Add 650 μL of 0.05% trypsin-EDTA to the 90% confluent dish of cells, tilting the dish to
117   evenly distribute the enzyme. Place the dish with the trypsin into the incubator for 1 minute.

118

119   1.7   Remove the dish with the cells from the incubator. Add 10 mL of cell culture media into a
120   15 mL centrifuge tube. Quickly add another 10 mL of media into the dish to quench the trypsin.

121

122   1.8   Pipette 1 mL of the trypsinized cells into the 15 mL centrifuge tube in order to dilute the
123   cells. Pipette the contents of the tube up and down to ensure an even distribution of cells within
124   the media. For cell types with high aggregation propensity, filtering cells through a cell strainer
125   (100 μm mesh size) is recommended to minimize the occurrence of cell clumping.

126

127   1.9   From the tube, pipette 500 - 1000 μL of diluted cells into the 35 mm dish containing the
128   coverslip.

129

130   1.10   Gently shake the dish to evenly spread out the cells. Ensure that the coverslip is at a ~10%
131   confluency (~50,000 cells/mL) and adjust the volume of diluted cells as needed.

132

133 NOTE: The purpose of having cells at such low confluency is to ensure that there are 1-2 polarized
134 cells in each field of view that will be used to focus the objective throughout the cell spreading
135 acquisition.
136
137 1.11   Passage 1/5 of the remaining cells in the 10 cm dish into one 6 cm dish per treatment
138 condition. Place the passaged dishes and the 35 mm dish with the coverslip into the incubator
139 overnight.
140
141 NOTE: These will be the cells that will be analyzed for spreading dynamics.
142
143 2.   **Drug Incubation and Cell Recovery**
144
145 2.1   Add 5 mL of cell culture media into each of two 15 mL centrifuge tubes, and 20 mL of
146 phenol red free DMEM into each of two 50 mL centrifuge tubes.
147
148 NOTE: The number of tube pairs (15 mL + 50 mL) should correspond to the number of
149 experimental conditions.
150
151 2.2   To test the importance of Arp2/3 for cell spreading, pipette either the pharmacological
152 inhibitor of Arp2/3, CK-666, or the control treatment, such as DMSO, into each pair of centrifuge
153 tubes up to the desired concentration.
154
155 2.3   Remove the passaged 6 cm dishes (see Step 1.11) from the incubator and aspirate the
156 media. Wash the dishes with warm PBS.
157
158 2.4   Add the contents of the CK-666- or DMSO-supplemented 15 mL centrifuge tubes into each
159 of the passaged dishes. Label each dish with the correct drug treatment and place the dishes into
160 the incubator for one hour.
161
162 2.5   Remove the dishes from the incubator and aspirate the media. Wash the dishes with
163 warm PBS in order to thoroughly remove all the remaining phenol red media.
164
165 2.6   Add 230 µL of 0.05% trypsin-EDTA to each 6 cm dish and incubate cells for 1 minute.
166
167 NOTE: If applicable, trypsin can be replaced by a non-proteolytic cell adhesion blocker.
168
169 2.7   Remove the dishes from the incubator. For each treatment, add 5 mL of drug-
170 supplemented phenol red free DMEM into a 15 mL centrifuge tube designated as "Tube B". Add
171 an additional 5 mL of the same media into the relevant dish to quench the trypsin. Transfer the
172 contents of the dish into a 15 mL centrifuge tube designated as "Tube A".
173
174 2.8   Transfer 1 mL of cells from Tube A into Tube B. Repeat for each treatment.
175

176 2.9   Place Tubes A and B into the incubator for 45 minutes to allow cells to recover from
177 trypsinization. Slightly loosen the cap of the centrifuge tubes before placing them in the incubator
178 to allow for CO_2 penetrance.

179
180 NOTE: The duration of recovery time may vary for different cell types. Although in our
181 experiments 45-minute-long recovery had a negligible effect on cell viability, some cell types may
182 undergo anoikis when maintained in suspension for too long. Therefore, we recommend
183 determining the optimal recovery time empirically. The optimal recovery time enables fast and
184 synchronous cell spreading with no dead or apoptotic cells in the sample.

185
186 3.   **Magnetic Chamber Preparation**

187
188 3.1   Ensure that all parts of a 1 Well Chamlide Cell Magnetic Chamber that can accommodate
189 a 22 mm x 22 mm square coverslip have been cleaned before use.

190
191 3.2   Remove the 35 mm dish with the coverslip (see Step 1.11) from the incubator. Aspirate
192 the cell culture media and wash the coverslip with warm PBS.

193
194 3.3   Remove the coverslip from the 35 mm dish using a pair of forceps and gently lay the
195 coverslip onto the bottom plate of the magnetic chamber.

196
197 3.4   Place the silicone gasket on top of the coverslip.

198
199 NOTE: An improperly placed silicone gasket is the most common cause of a leaky magnetic
200 chamber. Ensure that the gasket rests in the indent of the bottom plate and does not rise beyond
201 the indent.

202
203 3.5   Attach the main body onto the bottom plate.

204
205 NOTE: Do this part very slowly. A good tip is to hold down the bottom plate with one hand while
206 placing the main body on top. This ensures that the main body's magnets do not lift the bottom
207 plate up, which could potentially displace and crack the coverslip.

208
209 3.6   Add 1 mL of drug-supplemented phenol red free DMEM to the magnetic chamber. Take
210 a lint-free tissue and carefully dab the enclosure between the main body and the bottom plate
211 in order to check for any leaks.

212
213 NOTE: If there is leakage, quickly aspirate the media and proceed again from step 3.4.

214
215 3.7   Lower the transparent cover onto the main body to enclose the magnetic chamber.

216
217 3.8   Spray a laboratory tissue first with water and wipe the bottom of the magnetic chamber
218 (the coverslip, not the metal part). Afterwards, spray a second laboratory tissue with a small
219 amount of 70% ethanol and wipe, being careful not to crack the coverslip.

220

221 4.   **Image Acquisition**

222

223 4.1   Preheat the stage top incubator and the objective heater to 37 °C and set the CO_2 level in
224 the stage top incubator to 5%.

225

226 NOTE: If the stage top incubator is not connected to a CO_2 supply, the cell culture media should
227 be supplemented with 25 mM HEPES to maintain constant pH 7.4.

228

229 4.2   Apply a sufficient amount of immersion oil to the pre-warmed 60X, 1.4 N.A. oil objective.

230

231 NOTE: We use a 60X, 1.4 N.A. oil immersion objective in this protocol because of its reasonably
232 large field of view and outstanding light collection efficiency. If a larger field of view is required,
233 a lower magnification objective (*e.g.*, 20x) can be used as long as the signal-to-noise ratio of the
234 images is greater than 2.5.

235

236 4.3   Bring both the completed magnetic chamber and Tube B (Step 2.9) to the confocal
237 microscope. Place the magnetic chamber onto the stage top incubator.

238

239 NOTE: Place the magnetic chamber gently on the stage to avoid creating bubbles in the
240 immersion oil.

241

242 4.4   Set focus to the fluorescent cells using the GFP channel. Make sure that the cell edge is
243 sharp and well defined.

244

245 4.5   Remove the transparent cover of the magnetic chamber and pipette 500 μL from Tube B
246 into the magnetic chamber. Place the transparent cover back on top of the magnetic chamber.

247

248 4.6   To identify cells ideal for cell spreading analysis, search for "halos" of cells that have yet
249 to attach to the coverslip but are no longer rolling around. Cells that are in the earliest stages of
250 coverslip attachment are also great candidates, but image acquisition must be swift in order to
251 capture spreading.

252

253 4.7   Configure the time-lapse image acquisition for the green channel to include four fields of
254 view, imaged at 6 second intervals.

255

256 NOTE: Due to the high variability of lamellipodia protrusion velocity among different cell types,
257 the optimal frame rate should be determined empirically. The imaging interval of 6 seconds used
258 in our experiments is a good starting point for the analysis of many mesenchymal and epithelial
259 cells. However, cells that spread very quickly (*e.g.*, immune cells) may require a much higher
260 frame rate (shorter imaging interval). The optimal frame rate for cell spreading movies ensures a
261 2-5 pixels displacement of the protruding cell edge between subsequent frames. Considering the
262 accuracy of curve fitting used to identify the plateau of cell spreading, the optimal frame rate
263 should also ensure 50-100 measurements of cell edge displacement during the rapid expansion

264 phase of cell spreading. The number of fields of view should be adjusted depending on the
265 exposure time, the distance between acquisition points, and the stage movement speed. Users
266 are advised to determine the maximum number of fields of view that can acquired with the
267 desired frame rate.
268
269 4.8   After identifying a suitable field of view, save the X and Y coordinates of the microscope
270 stage. Proceed with identifying three other fields of view that are relatively close to one another
271 on the coverslip. Save the coordinates of the microscope stage for every desired field of view.
272
273 NOTE: It is strongly recommended to optimize the stage movement path between fields of view
274 in order to minimize any unnecessary sample movement. Such optimization can be performed
275 either manually or automatically. Excessive sample movement slows down the acquisition and
276 may cause cells to roll out of view as they are descending.
277
278 4.9   Acquire images for 15 minutes at a 6 second frame rate and save the files. If more
279 acquisitions are required, repeat starting at Step 4.6.
280
281 **5.   Analysis of cell area, circularity and protrusion dynamics during cell spreading**
282
283 5.1   Prepare images for data processing and analysis
284
285 NOTE: The software requires an image in .tiff format and a pixel size as the input parameters.
286 Both requirements can be fulfilled using the acquisition software or Fiji (in this protocol). If these
287 requirements are fulfilled, proceed to step 5.2.
288
289 5.1.1   Install the latest version of Fiji application (https://imagej.net/Fiji/Downloads).
290
291 5.1.2   Open a time-lapse image using Fiji.
292
293 5.1.3   Copy the pixel size of the image by selecting **Image > Properties**. Copy and paste the pixel
294 size in μm to Notepad/Word.
295
296 5.1.4   For the analysis of cell spread area and circularity, save the time-lapse image as a tiff
297 image stack. The custom-build analysis software does not support proprietary file formats. Save
298 the individual cell tiff image stack by selecting **File > Save As > Tiff**.
299
300 5.2   Install the Python IDE (Spyder) and the necessary packages (**PySimpleGUI** and **tifffile**) for
301 data processing and analysis.
302
303 NOTE: The installation of Python and packages is only required for the initial setup.
304
305 5.2.1   The time-lapse movies will be analyzed in the Spyder IDE using a custom-build Python
306 script.   To   download   the   Spyder   IDE,   download   the   Anaconda   distributor

(https://www.anaconda.com/products/individual) which includes Spyder IDE and most of the
308 necessary libraries and packages for this analysis.

309

310 5.2.2   Install Anaconda and launch Spyder through Anaconda Navigator.

311

312 5.2.3   In the IPython console tab (located in the lower right section of Spyder), copy and paste
313 the following command: **pip install PySimpleGUI** and press the enter key. Running this command
314 will install the package needed to initiate the graphical user interface (GUI).

315

316 5.2.4   In the same console, copy and paste the following command: **pip install tifffile** and press
317 the **Enter** key. Running this command will install the package needed to save images as tiff files.

318

319 5.2.5   Download all the Python scripts from the supplemental files or the most updated scripts
320 from GitHub at: https://github.com/ernestiu/Cell-spreading-analysis.git

321

322 5.3   Quantify cell area and cell shape factors during cell spreading

323

324 5.3.1   Open the main analysis script "cell_spreading_GUI.py" by selecting the open file option
325 in the top panel of Spyder or using the shortcut **Ctrl + O**.

326

327 5.3.2   Open the cell spreading analysis GUI by selecting "Run file" in the top panel or using the
328 shortcut **F5**.

329

330 5.3.3   Click the **Cell Spread Area** tab (**Figure 3A**).

331

332 5.3.4   Select the tiff image to be analyzed using the browse button.

333

334 NOTE: The selected file must be a tiff file.

335

336 5.3.5   Specify the destination directory where data outputs (e.g., cell masks, values) will be
337 saved.

338

339 5.3.6   Specify the data output settings:

340

341 5.3.6.1. Save masks: Save cell masks generated during the segmentation process.

342

343 5.3.6.2. Export data: Export an excel spreadsheet (.xlsx) that contains all the analysis data to the
344 destination folder.
345 Cell area, circularity and aspect ratio of all spreading cells will be saved as an Excel spreadsheet
346 in the destination folder. The cell area is calculated as:
347 $\square\square\square\square\ \square\square\square\square\ (\square\square^2) = \square\square\square\square\square\square\square\ \square\square\ \square\square\square\square\square\square\square \times \square\square\square\square\square\ \square\square\square\square\ (\square\square^2)$ (1)
348 The cell circularity is a measure of how close a cell is to a perfectly round cell. It is calculated as:
349 $\square\square\square\square\ \square\square\square\square\square\square\square\square\square\square\square\square\square = \frac{4\times\square\times\square}{\square^2}$ (2)

350 where A and P are the cell area and the cell perimeter, respectively. The aspect ratio of the cell
351 represents how elongated the cell is. A spreading cell should have an aspect ratio close to 1. The
352 aspect ratio is calculated as:

353 $\square\square\square\square\square\square\ \square\square\square\square\square = \frac{\square\square\square\square\square\ \square\square\square\square\ \square\square\square\square\square\square}{\square\square\square\square\square\ \square\square\square\square\ \square\square\square\square\square\square}$ (3).

355 5.3.6.3. Save contours: Save the cell boundary contour overlay images in the destination folder.

357 5.3.7 Specify the segmentation settings:

359 5.3.7.1. Show segmentation: Show the segmentation result in the Spyder console during the
360 analysis process.

362 5.3.7.2. Smallest cell area (μm^2): Enter the minimum value for cell area, including area values of
363 cells in the beginning stages of attachment. Objects with an area smaller than this threshold will
364 not be considered as spreading cells. This number will affect the segmentation process.

366 5.3.8 Specify the image parameters.

368 5.3.8.1. Acquisition interval (s): Enter the frequency of the image acquisition in seconds.

370 5.3.8.2. Pixel size (μm): Enter the pixel size that was recorded when preparing images for analysis.

372 5.3.8.4. Image bit depth: Enter the bit depth of the camera/detector.

374 5.3.9 Click **Run**. If an error arises, an error message will appear in Spyder's console. Otherwise,
375 the image analysis process will be shown in the console.

377 NOTE: The first image to appear in the console/Plots section (depending on the Spyder settings)
378 shows all the cells identified in the field of view. Green boxes placed around the cells indicate
379 spreading cells that are suitable for segmentation and analysis. Grey boxes indicate cells that are
380 not suitable for analysis. The total number of identified spreading cells will also appear in the
381 Console tab. The software plots the cell area (in blue) and cell circularity (in red) as a function of
382 time. These graphs allow users to evaluate the accuracy of cell segmentation. A successful
383 segmentation yields a monotonically increasing curve for cell area. To obtain a representative
384 curve of cell spread area, the lag phase should be removed from the graph manually. The lag
385 phase includes measurements of cell area before the cell starts spreading. The lag phase is
386 indicated by fast fluctuations, as represented in the cell area plot (Figure 3C right).

388 **6.   Quantify cell edge dynamics during cell spreading using kymographs**

390 6.1   Prior to running the analysis, crop the raw movies of spreading cells to create time series
391 of individual spreading cells.

393   6.1.1   Use the **Rectangle** tool in the Fiji tool bar to manually select a region of interest (ROI) that
394   encapsulates **a single cell**. (To ensure that the ROI fully encapsulates the spreading cell, use the
395   scroll function to inspect the ROI at all time points.)
396
397   6.1.2   Right click on the ROI and select **Duplicate**.
398
399   6.1.3   Check **Duplicate stack** and click **OK**.
400
401   6.2   Open the main analysis script "cell_spreading_GUI.py" by selecting the **Open File** button
402   in Spyder's tool bar or using the shortcut **Ctrl** + **O**. If the GUI has already been opened, go directly
403   to Step 6.3.
404
405   6.3   Open the cell spreading analysis GUI by selecting **Run file** in the top panel or using the
406   shortcut **F5** (**Figure 3B**).
407
408   6.4   Click the **Kymograph generator & analysis** tab.
409
410   6.5   Use the browse button to select the tiff image for the analysis.
411
412   NOTE: Proprietary file formats, *e.g.,* nd2, lif, zen, are not supported by the script)
413
414   6.6   Specify the destination folder to save the output data (cell masks and values).
415
416   6.7   Specify the output settings.
417
418   6.7.1. Export data: Export an excel spreadsheet (.xlsx) to the destination folder that contains
419   relative cell edge positions and retraction events of the kymographs.
420
421   6.8   Specify the image parameters:
422
423   6.8.1. Acquisition interval (s): Enter the image acquisition frequency in seconds.
424
425   6.8.2. Pixel size (µm): Enter the pixel size that was recorded when preparing images for the
426   analysis in Step 5.1.3.
427
428   6.8.3. Smallest cell area (µm^2): Enter the minimum value for cell area, including area values of
429   cells in the beginning stages of attachment. Objects with an area smaller than this threshold will
430   not be considered as spreading cells. This number will affect the segmentation process.
431
432   6.8.4. Image bit depth: Enter the bit depth of the camera/detector.
433
434   6.9   Click **Run**. If an error arises, an error message will appear in Spyder's console. Otherwise,
435   a summary of the protrusion dynamics quantifications will be shown in the console. There will be
436   4 pairs of retraction frequency and protrusion speed measurements, which are extracted from 4

437 kymographs generated from the top, bottom, left and right portions of the cell. The retraction
438 frequency   is   calculated   as:
439 $Retraction\ frequency\ (s^{-1}) = \dfrac{The\ number\ of\ local\ minima}{The\ length\ of\ protrusion\ phase\ (s)}$ (4).
440
441 NOTE: This number demonstrates how frequently the lamellipodium retracts over the course of
442 spreading. The average protrusion speed is measured by measuring the slope between the
443 beginning of protrusion and the plateau point on the kymograph. A summary kymograph figure
444 will be shown in the console after the segmentation. To save the summary figure, right click on
445 the figure and save the image.
446
447 **REPRESENTATIVE RESULTS:**
448 The above protocol describes the experimental procedures for the live-cell imaging of spreading
449 cells and a computational tool for the quantitative analysis of cell spreading dynamics. The
450 computational tool can be used in a low- or high-throughput format to identify the molecular
451 players regulating the actin polymerization machinery at the cell leading edge.
452
453 The schematic representation of the experimental procedures is depicted in **Figure 1**. The cell
454 spreading assay was performed on immortalized mouse embryo fibroblasts stably expressing the
455 pleckstrin homology (PH) domain of the Akt protein kinase tagged with eGFP[25]. The cells were
456 detached with trypsin-EDTA and were allowed to recover in suspension for 45 minutes. During
457 the recovery step, cells replenished their integrin receptors on the plasma membrane as
458 indicated by the fast and synchronous attachment of the recovered cells to the fibronectin coated
459 coverslips (**Figure 2**). Without the recovery, cells spread for 15 minutes exhibited a broad
460 distribution of cell size indicating a high variability in the onset of cell spreading (**Figure 2A and
461 B**). Next, cells were plated on a fiducially-marked coverslip and their spreading dynamics were
462 visualized by spinning disk confocal microscopy (**schematics shown in Figure 1A – H**). Throughout
463 the image acquisition, we considered fields of view that featured cells with a signal-to-noise ratio
464 of 2.5 or above. This was an important consideration as the subsequent image segmentation is
465 sensitive to the cells' fluorescence intensity relative to the background. In our experiments, we
466 acquired images every 6 seconds for 15 minutes (**schematics shown in Figure 1I-J**). In agreement
467 with previous reports[16], imaging at a 6 second frame rate ensured sufficient temporal resolution
468 for capturing the dynamics of individual protrusion and retraction events, while allowing us to
469 acquire several fields of view in parallel. The resulting time-lapse images were analyzed using the
470 custom-build Python software (**Figure 3**).
471
472 An unbiased quantification of cell spreading was performed by using two distinct analytical
473 procedures: (*i*) Morphodynamic profiling of spreading cells (**Figure 3A, C and 4**) and (*ii*)
474 Kymograph analysis of cell edge dynamics (**Figure 3B and 5**). The analysis of cell spreading by
475 morphodynamic profiling involves the automated detection of the spreading and fiducial cells in
476 the field of view (**Figure 3C left**), followed by a frame-by-frame image segmentation and
477 detection of the spreading cell boundary. The segmentation is performed by global intensity
478 thresholding the individual frames. The threshold value is calculated as the local minimum
479 between the first and second intensity modes on the image histogram[26]. Images with a unimodal,

480 right-skewed histogram are segmented by the triangle thresholding algorithm[27]. Following cell
481 segmentation, the morphodynamic characteristics of the spreading cells (*i.e.,* cell area, aspect
482 ratio, and cell circularity) were computed (**Figure 3C right**).
483
484 Consistent with published results[12, 28], cell spreading was driven by an isotropic expansion of
485 lamellipodia as indicated by a sigmoidal shape on the representative cell area plot (**Figure 3C**
486 **right, blue curve and S1**)**.** The area plot showed that the cell area increased by approximately 3-
487 fold before reaching a plateau (**Figure 4A and B**). Throughout the process of cell spreading, the
488 cells remained circular (circularity = 0.70 ± 0.076) and displayed veil-like protruding cell edges,
489 which are indicative of lamellipodial protrusions (**Figure 4C**).
490
491 To validate the cell spreading assay, we inhibited Arp2/3 with 100 µM CK-666 for 1 hour and 45
492 minutes and determined the effect of this treatment on the cell spreading dynamics. In
493 agreement with previous reports[13], the suppression of Arp2/3 activity did not result in a
494 significant decrease in the cell spreading speed (**Figure 4A and B, pink curve**)**.** However, cell
495 shape analysis revealed a significant difference in the circularity of control and CK-666 treated
496 cells (Control: 0.70 ± 0.08 vs. CK-666: 0.54 ± 0.09, $p < 0. 1 \times 10^{-3}$) (**Figure 4C**). While the control
497 cells remained circular until the plateau, Arp2/3-inhibited cells acquired a polygonal shape which
498 was retained throughout the course of spreading (**Figure 4A**). Together, these experimental
499 results demonstrate that the described cell spreading assay reveals moderate changes in cell
500 morphodynamics caused by perturbations of the actin polymerization machinery.
501
502 While morphodynamic profiling is often sufficient to detect gross alterations in cell spreading
503 dynamics, this analysis has limited ability to identify specific cytoskeletal components that
504 regulate the protrusion-retraction cycles of the cell edge, prompting us to implement an
505 unbiased Kymograph Analysis tool (**Figure 5 left, dashed lines**). The analysis of cell edge speed
506 revealed a moderate but significant decrease in the average protrusion speed of Arp2/3-inhibited
507 cells compared to control (Control: 37.1 ± 12.87 nm/s vs. CK-666: 28.7 ± 13.4 nm/s, $p = 0. 9 \times 10^{-3}$)
508 (**Figure 5C**). Furthermore, dynamics of the cell edge of control and Arp2/3-inhibited cells were
509 remarkably different (**Figure 5A and D**). The control cells protruded persistently with little to no
510 retractions during the rapid expansion phase, which lasted about 200 seconds, and exhibited
511 intermittent retractions during the plateau phase (**Figure 5A and D**). In contrast, the expansion
512 of Arp2/3-inhibited cells was intervened by retraction events, denoted by the red dots on the
513 graphs (**Figure 5B and D**). Quantification of retraction frequency showed that Arp2/3-inhibited
514 cells retracted 26% more frequently than control cells (Control: 0.18 ± 0.22 s^{-1} vs. CK-666: 0.24
515 ± 0.19 s^{-1}, p = 0.03) (**Figure 5D**). These data demonstrate the high sensitivity of the kymograph
516 analysis in detecting mild alterations in lamellipodial dynamics.
517
518 **FIGURE AND TABLE LEGENDS:**
519 **Figure 1: The experimental workflow of a cell spreading assay.** (**A - H**) Schematics of the cell
520 spreading assay. (**A**) A 22 mm x 22 mm coverslip is coated with fibronectin diluted in PBS to a
521 final concentration of 2.5 µg/mL. (**B**) A confluent 10 cm dish of PH-Akt-GFP-expressing mouse
522 embryonic fibroblasts (MEFs) is washed with PBS and treated with 0.05% trypsin-EDTA. The
523 trypsin-treated cells are then split into a 15 mL centrifuge tube and a 6 cm tissue culture dish,

both containing cell culture media. (**C**) From the 15 mL centrifuge tube, 500-1000 µL is pipetted onto the fibronectin-coated coverslip. (**D**) The 6 cm dish and the 35 mm dish with the coverslip containing the sparsely seeded cells are placed in a 37 °C incubator overnight. Once polarized, these cells will provide the frame of focus for the cell spreading acquisition. (**E**) An hour before image acquisition, the 6 cm dish's media is replaced with phenol-red free DMEM supplemented with HEPES and the drug of interest. After 1 hour, the cells are treated with 0.05% trypsin-EDTA and transferred to a 15 mL centrifuge tube (Tube A) containing the HEPES/drug-supplemented phenol red free DMEM. The cells in Tube A are then further diluted in another 15 mL centrifuge tube (Tube B), which is placed in the incubator for 45 minutes. (**F**) As the cells recover, the magnetic chamber is prepared from bottom to top: first the bottom plate is placed on a flat surface, then the coverslip with the polarized cells, the silicone gasket, the main body of the chamber, and finally the transparent cover are laid on top. (**G**) 1 mL of drug-supplemented phenol red free DMEM is pipetted into the magnetic chamber, which is then brought to the microscope stage. A CFI Plan Apo Lambda 60X Oil objective is selected for image acquisition. (**H**) The transparent cover is removed and 500 µL of Tube B's contents are pipetted into the magnetic chamber. (**I**) For image acquisition, appropriate fields of view will contain green "halos", which are suspended cells that have not yet attached to the coverslip. (**J**) The cells are imaged for 15 minutes.

Figure 2: The effect of recovery time on cell spreading. Cells maintained in suspension for the indicated time (cell recovery step in the protocol) were plated on fibronectin-coated coverslips for 15 minutes, fixed with 4% paraformaldehyde and imaged by phase contrast microscopy. (**A**) Top panels: phase contrast images acquired with a 20X objective. Bottom panels: watershed-segmented cell masks with the cell areas color-coded. (**B**) Quantification of cell area.

Figure 3: Graphical User Interface (**GUI**) **and the working principles of image processing and analysis software.** (**A**) The GUI of the "Cell spread area" tab. Refer to Step **5.3** for instructions. (**B**) The GUI of the "Kymograph generator & analysis" tab. Refer to Step **6** for instructions. (**C**) The image processing pipeline of the software. The software first identifies spreading cells (labeled by a green bounding box) in the whole field of view. The spreading cells are identified based on their intensity value, circularity, and aspect ratio. The identified spreading cells are then segmented frame-by-frame using global intensity thresholding. Each binary mask is processed by median filtering and binary hole filling followed by morphological closing to smoothen the cell edge. The red outline corresponds to the segmented cell boundary. The cell's area, aspect ratio, and circularity are extracted from the binary cell map. The graph shows the area and circularity of a representative cell over time. Upon cell seeding, cells do not start spreading immediately, giving rise to the lag phase seen on the graph. Following the lag phase, cells spread rapidly during the rapid expansion phase and eventually reach a plateau phase.

Figure 4: Representative results of cell spread area analysis upon Arp2/3 inhibition. (**A**) Representative images of PH-Akt-GFP-expressing MEFs spreading on a fibronectin-coated coverslip over the course of 3 minutes. The red line indicates the cell boundary extracted by the cell segmentation algorithm. Top panels: 0.1% DMSO-treated cells. Bottom panels: 100 µM CK-666 (Arp2/3 inhibitor)-treated cells. (**B**) A graph showing cell spread area over time. The cell

568 spread area was quantified as fold changes relative to the average cell spread area of control
569 cells. Blue and pink lines represent control and Arp2/3-inhibited cells, respectively. The shaded
570 regions indicate the upper and lower standard deviation of the cell spread area. (**C**) A bar plot
571 with individual data points showing the average cell circularity of control and Arp2/3-inhibited
572 cells. All error bars represent standard deviation. *, $p < 0.05$, **, $p < 0.01$, ***, $p < 0.001$, n.s. (not
573 significant, $p > 0.05$) as detected by parametric student t-tests.

575 **Figure 5: Representative results of kymograph analysis of spreading cells upon Arp2/3**
576 **inhibition.** (**A – B**) Representative images and kymographs extracted from 0.1% DMSO-treated
577 (control) cells and 100 µM CK-666 (Arp2/3 inhibitor)-treated cells. Left panels: inverted grayscale
578 images of a control and Arp2/3-inhibited cell. The dashed lines correspond to the pre-defined
579 lines where kymographs were extracted. Right panels: kymographs are extracted along the
580 dashed lines shown on the grayscale images. The plot boundaries are color-coded to match the
581 dashed lines on the grayscale images. The dashed line in each plot indicates the slope of the curve
582 from which the average protrusion speed was calculated. To pinpoint the plateau phase, a logistic
583 growth curve was fitted to the data points and the plateau was derived from the parameter, c
584 (**Supplementary Figure 1**). The red dots denote the retraction events. (**C**) A bar plot with
585 individual data points showing the average protrusion speeds of the control and Arp2/3-inhibited
586 cells. All error bars represent standard deviation. (**D**) A bar plot with individual data points
587 showing the frequency of retraction events of the control and Arp2/3-inhibited cells. (**C – D**) *, p
588 < 0.05, **, $p < 0.01$, ***, $p < 0.001$, n.s. (not significant, $p > 0.05$) as detected by non-parametric
589 Mann-Whitney tests.

591 **Supplemental Figure 1: A representative kymograph and the curve fitting result.** A kymograph
592 extracted from a spreading cell. The blue dashed line corresponds to the distance of the cell edge
593 relative to the first frame. The red solid line corresponds to the fitted curve. To increase the
594 confidence of the curve fitting, the raw data points were first smoothed by a Savitzky-Golay filter.
595 After the curve-fitting, the parameter c, from the logistic equation, was used to identify the
596 plateau point. The raw data point closest to c is designated as the plateau point.

598 **DISCUSSION:**
599 The described cell spreading assay allows for the continuous tracking of morphological changes
600 (*e.g.,* cell size and shape) and cell edge movements (*i.e.,* protrusion speed and retraction
601 frequency), which are features missing in most cell spreading protocols[19, 24]. While commonly
602 used end-point cell spreading assays allow for the determination of cell spreading speed, these
603 assays fail to resolve the temporal dynamics of cell edge movements. The lack of temporal
604 information limits the ability to detect and quantify changes in lamellipodial protrusion-
605 retraction cycles.

607 Our image processing and analysis software performs a streamlined analysis of the spreading
608 cells, from cell segmentation to data quantification. Manual image analyses of cell spreading
609 usually involve biased selection of a threshold value or applying an automated segmentation
610 algorithm, which is not suited for high-throughput experiments where many images need to be
611 analyzed. Our software is, therefore, designed to detect and segment spreading cells in an

612 automatic fashion, in addition to quantifying protrusion dynamics and morphological descriptors.
613 Together, these features make the described protocol amenable for large-throughput screenings
614 of signaling pathways and molecular players that regulate lamellipodia.
615
616 To ensure that the analysis of spreading cells is robust and accurate, a few critical steps in the
617 protocol must be performed with extra caution. The first step of the cell spreading assay involves
618 plating fluorescently-labeled cells at a very low density on a fibronectin-coated coverslip the day
619 before imaging (**Figure 1A-D**). These polarized cells enable precise focusing of the spreading cells'
620 protruding edges during the image acquisition. If the density of polarized cells is too high,
621 spreading cells have a high chance of landing on or overlapping with the polarized cells, which
622 may lead to a cell segmentation failure. The recovery period post-trypsinization is another critical
623 step in this protocol. Cells treated with the drug of interest, *e.g.,* DMSO or CK-666, are detached
624 from the cell culture dish by trypsin-EDTA (Step 2), followed by a recovery period of 45 mins
625 (**Figure 1E**). This recovery step allows cells to recover from the proteolytic cleavage of cell surface
626 proteins by trypsin[19, 24] and synchronizes the onset of cell spreading (**Figure 2**). If the recovery
627 step is omitted, the cell-to-cell variability in cell spread area increases, reducing the consistency
628 of the biological phenotype.
629
630 During the image acquisition, any sample drift inevitably decreases the quality and precision of
631 cell spreading analysis, especially the kymograph analysis. To minimize sample drift, a few
632 measures should be taken. First, the user should optimize the stage movement during the image
633 acquisition. The optimization includes minimizing stage travel between fields of view and
634 reducing the speed of stage movement. Second, it is essential to tightly secure the sample on the
635 microscope stage. If these suggested measures do not eliminate sample drift, post-acquisition
636 processing should be considered. Among many proprietary and open-source computational
637 tools, we recommend using the "Descriptor-based registration" Fiji plugin to correct image shifts
638 and align the movies of spreading cells (instructions can be found at:
639 https://imagej.net/Descriptor-based_registration_(2d/3d)).
640
641 It should be noted that the quantitative analysis of cell areas and edge dynamics performed by
642 the software depends heavily on the accuracy of cell segmentation. To ensure precise
643 segmentation, we recommend visualizing cell spreading using a confocal imaging system,
644 preferably a spinning disk confocal microscope which offers high resolution, low
645 photobleaching/phototoxicity, and high signal-to-noise ratio. A confocal microscope efficiently
646 removes out-of-focus fluorescence emitted by the spreading cells, which would otherwise
647 decrease the image segmentation accuracy and cell boundary tracing. If a widefield microscope
648 is used for image acquisition, additional post-acquisitional processing, *e.g.,* image deconvolution,
649 may be required to remove out-of-focus fluorescence and improve the accuracy of cell
650 segmentation. Therefore, the choice of the imaging system should be considered.
651
652 Within the described software, two image segmentation algorithms were implemented and
653 optimized to reliably detect cells labeled with dim to moderately bright fluorescent proteins, such
654 as cytosolic green and red fluorescent proteins (GFP and RFP)[26, 27]. However, these segmentation
655 algorithms have a limited dynamic range and are not suitable for detecting cells labeled with

extremely bright fluorescent proteins or dyes. In our hands, these algorithms tend to undersegment extremely bright cells due to the skewness of the image histogram towards high intensity pixels. For bright samples, the intensities of the images can be controlled by adjusting the exposure time or the output power of the excitation laser.

With these considerations in mind, this live-cell spreading protocol is a robust and powerful tool to study the dynamics of lamellipodia. The automated image analysis platform is suited to many biological investigations, *e.g.,* high-content screening of molecular/signaling factors that regulate lamellipodial protrusions.

DISCLOSURES:
The authors have nothing to disclose.

REFERENCES:
1. Mullins, R.D., Heuser, J.A., Pollard, T.D. The interaction of Arp2/3 complex with actin: Nucleation, high affinity pointed end capping, and formation of branching networks of filaments. *Proceedings of the National Academy of Sciences*. **95** (11), 6181–6186, doi: 10.1073/pnas.95.11.6181 (1998).
2. Yang, C., Czech, L., Gerboth, S., Kojima, S., Scita, G., Svitkina, T. Novel Roles of Formin mDia2 in Lamellipodia and Filopodia Formation in Motile Cells. *PLoS Biology*. **5** (11), e317, doi: 10.1371/journal.pbio.0050317 (2007).
3. Mogilner, A., Oster, G. Cell motility driven by actin polymerization. *Biophysical Journal*. **71** (6), 3030–3045, doi: 10.1016/s0006-3495(96)79496-1 (1996).
4. Mogilner, A., Oster, G. Force Generation by Actin Polymerization II: The Elastic Ratchet and Tethered Filaments. *Biophysical Journal*. **84** (3), 1591–1605, doi: 10.1016/s0006-3495(03)74969-8 (2003).
5. Pollard, T.D., Borisy, G.G. Cellular Motility Driven by Assembly and Disassembly of Actin Filaments. *Cell*. **112** (4), 453–465, doi: 10.1016/s0092-8674(03)00120-x (2003).
6. Wu, C. *et al.* Arp2/3 is critical for lamellipodia and response to extracellular matrix cues but is dispensable for chemotaxis. *Cell*. **148** (5), 973–87, doi: 10.1016/j.cell.2011.12.034 (2012).
7. Steffen, A. *et al.* Rac function is crucial for cell migration but is not required for spreading and focal adhesion formation. *Journal of cell science*. **126** (Pt 20), 4572–88, doi: 10.1242/jcs.118232 (2013).
8. Gupton, S.L. *et al.* Cell migration without a lamellipodium. *The Journal of Cell Biology*. **168** (4), 619–631, doi: 10.1083/jcb.200406063 (2005).
9. Dimchev, V. *et al.* Induced Arp2/3 Complex Depletion Increases FMNL2/3 Formin Expression and Filopodia Formation. *Frontiers in Cell and Developmental Biology*. **9**, 634708, doi: 10.3389/fcell.2021.634708 (2021).

700   10.   Leithner, A. *et al.* Diversified actin protrusions promote environmental exploration but
701   are dispensable for locomotion of leukocytes. *Nature cell biology*. **18** (11), 1253–1259, doi:
702   10.1038/ncb3426 (2016).
703   11.   Giannone, G., Dubin-Thaler, B.J., Döbereiner, H.-G., Kieffer, N., Bresnick, A.R., Sheetz,
704   M.P. Periodic Lamellipodial Contractions Correlate with Rearward Actin Waves. *Cell*. **116** (3), 431–
705   443, doi: 10.1016/s0092-8674(04)00058-3 (2004).
706   12.   Dubin-Thaler, B.J. *et al.* Quantification of Cell Edge Velocities and Traction Forces Reveals
707   Distinct Motility Modules during Cell Spreading. *PLoS ONE*. **3** (11), e3735, doi:
708   10.1371/journal.pone.0003735 (2008).
709   13.   Suraneni, P., Rubinstein, B., Unruh, J.R., Durnin, M., Hanein, D., Li, R. The Arp2/3 complex
710   is required for lamellipodia extension and directional fibroblast cell migration. *The Journal of cell
711   biology*. **197** (2), 239–51, doi: 10.1083/jcb.201112113 (2012).
712   14.   Wang, C. *et al.* Deconvolution of subcellular protrusion heterogeneity and the underlying
713   actin regulator dynamics from live cell imaging. *Nature Communications*. **9** (1), 1688, doi:
714   10.1038/s41467-018-04030-0 (2018).
715   15.   Dimchev, G. *et al.* Lamellipodin tunes cell migration by stabilizing protrusions and
716   promoting adhesion formation. *Journal of cell science*. **133** (7), jcs239020, doi:
717   10.1242/jcs.239020 (2020).
718   16.   Burnette, D.T. *et al.* A role for actin arcs in the leading-edge advance of migrating cells.
719   *Nature cell biology*. **13** (4), 371–81, doi: 10.1038/ncb2205 (2011).
720   17.   Yamada, K.M., Kennedy, D.W. Dualistic nature of adhesive protein function: fibronectin
721   and its biologically active peptide fragments can autoinhibit fibronectin function. *The Journal of
722   Cell Biology*. **99** (1), 29–36, doi: 10.1083/jcb.99.1.29 (1984).
723   18.   Cai, Y. *et al.* Nonmuscle Myosin IIA-Dependent Force Inhibits Cell Spreading and Drives F-
724   Actin Flow. *Biophysical Journal*. **91** (10), 3907–3920, doi: 10.1529/biophysj.106.084806 (2006).
725   19.   Humphries, M.J. Cell adhesion assays. *Molecular Biotechnology*. **18** (1), 57–61, doi:
726   10.1385/mb:18:1:57 (2001).
727   20.   Cavalcanti-Adam, E.A., Volberg, T., Micoulet, A., Kessler, H., Geiger, B., Spatz, J.P. Cell
728   Spreading and Focal Adhesion Dynamics Are Regulated by Spacing of Integrin Ligands. *Biophysical
729   Journal*. **92** (8), 2964–2974, doi: 10.1529/biophysj.106.089730 (2007).
730   21.   Dubin-Thaler, B.J., Giannone, G., Döbereiner, H.-G., Sheetz, M.P. Nanometer Analysis of
731   Cell Spreading on Matrix-Coated Surfaces Reveals Two Distinct Cell States and STEPs. *Biophysical
732   Journal*. **86** (3), 1794–1806, doi: 10.1016/s0006-3495(04)74246-0 (2004).
733   22.   Gauthier, N.C., Fardin, M.A., Roca-Cusachs, P., Sheetz, M.P. Temporary increase in plasma
734   membrane tension coordinates the activation of exocytosis and contraction during cell
735   spreading. *Proceedings of the National Academy of Sciences*. **108** (35), 14467–14472, doi:
736   10.1073/pnas.1105845108 (2011).
737   23.   Wolfenson, H., Iskratsch, T., Sheetz, M.P. Early Events in Cell Spreading as a Model for
738   Quantitative Analysis of Biomechanical Events. *Biophysical Journal*. **107** (11), 2508–2514, doi:
739   10.1016/j.bpj.2014.10.041 (2014).
740   24.   Guan, J.-L., Berrier, A.L., LaFlamme, S.E. Cell Migration, Developmental Methods and
741   Protocols. *Methods in molecular biology (Clifton, N.J.)*. **294**, 55–68, doi: 10.1385/1-59259-860-
742   9:055 (2004).
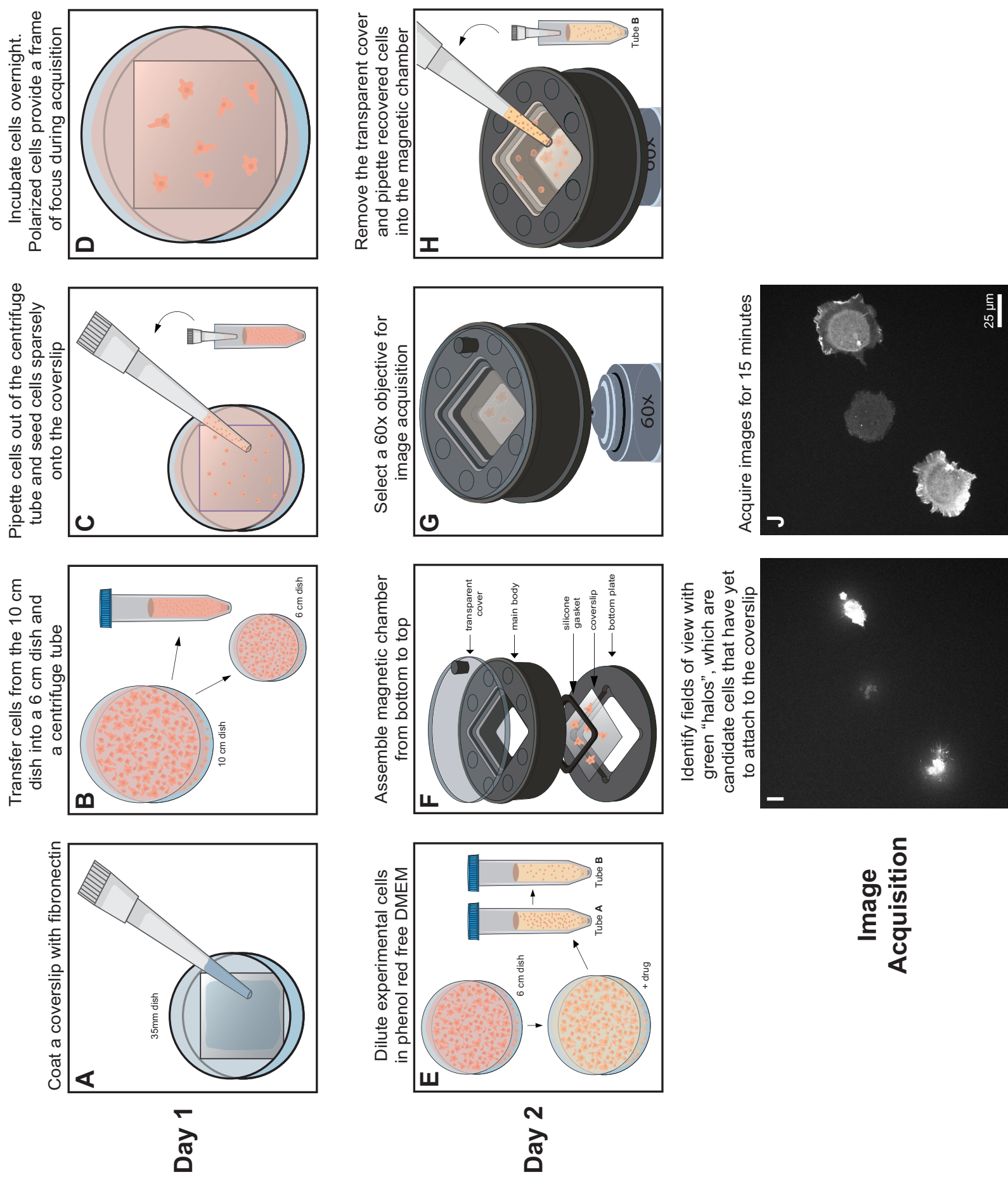743   25.   Raucher, D. *et al.* Phosphatidylinositol 4,5-Bisphosphate Functions as a Second

Messenger that Regulates Cytoskeleton–Plasma Membrane Adhesion. *Cell*. **100** (2), 221–228, doi: 10.1016/s0092-8674(00)81560-3 (2000).
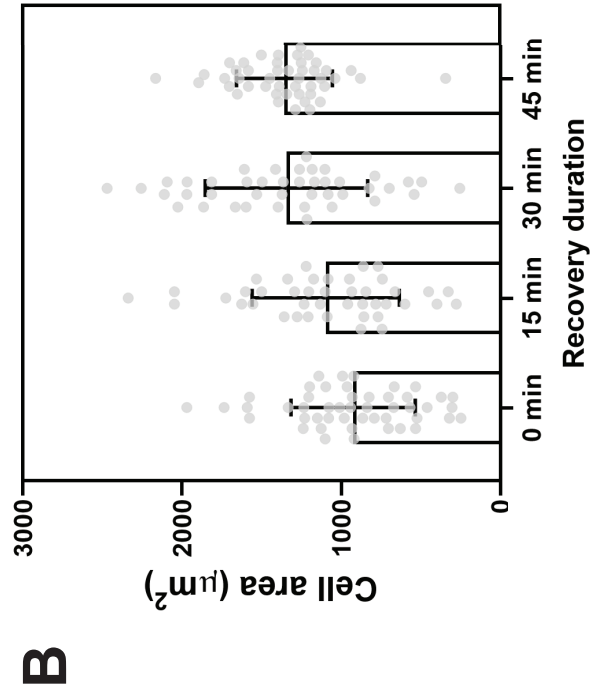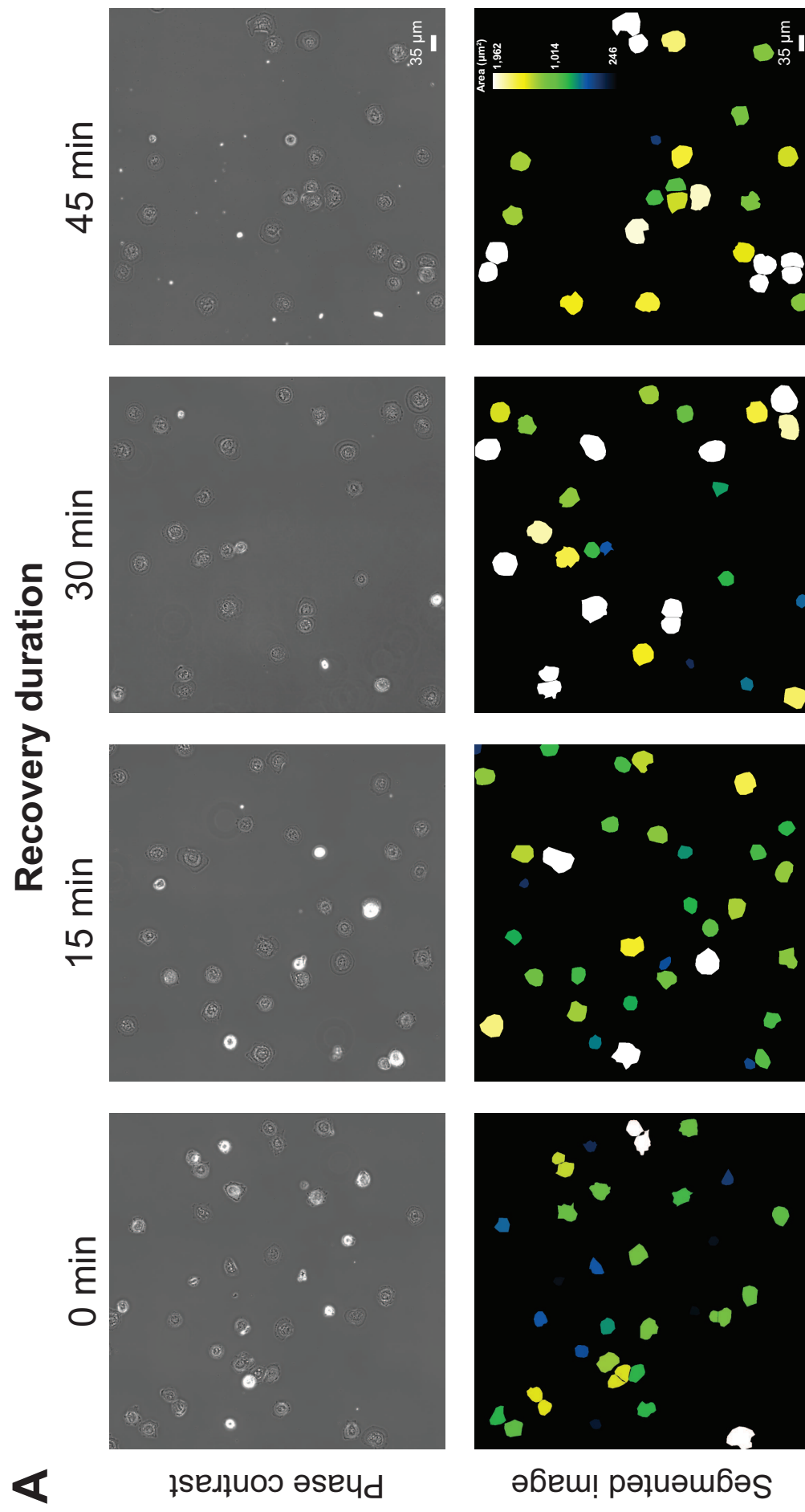
26.   Machacek, M., Danuser, G. Morphodynamic Profiling of Protrusion Phenotypes. *Biophysical Journal*. **90** (4), 1439–1452, doi: 10.1529/biophysj.105.070383 (2006).

27.   Zack, G.W., Rogers, W.E., Latt, S.A. Automatic measurement of sister chromatid exchange frequency. *The journal of histochemistry and cytochemistry : official journal of the Histochemistry Society*. **25** (7), 741–753, doi: 10.1177/25.7.70454 (1977).

28.   Bardsley, W.G., Aplin, J.D. Kinetic analysis of cell spreading. I. Theory and modelling of curves. *Journal of cell science*. **61**, 365–73 (1983).

Day 1

A. Coat a coverslip with fibronectin

B. Transfer cells from the 10 cm dish into a 6 cm dish and a centrifuge tube

C. Pipette cells out of the centrifuge tube and seed cells sparsely onto the coverslip

D. Incubate cells overnight. Polarized cells provide a frame of focus during acquisition

Day 2

E. Dilute experimental cells in phenol red free DMEM

F. Assemble magnetic chamber from bottom to top

G. Select a 60x objective for image acquisition

H. Remove the transparent cover and pipette recovered cells into the magnetic chamber

Image Acquisition

Identify fields of view with green "halos", which are candidate cells that have yet to attach to the coverslip

J. Acquire images for 15 minutes

25 µm

Figure

A

Cell Spreading Analysis

Cell spread area | Kymograph generator & analysis

Image location   [Browse]

Save data to   [Browse]

Output settings:
☐ Save masks
☑ Export data
☐ Save contours

Segmentation settings:
☐ Show segmentation (will take longer)

Smallest cell area (um^2):   (Try 33 um^2)

Image parameters:
Acquisition interval (s):
Pixel size (um):
Image bit depth: 8 / 12 / 16

[Run] [Cancel]

Last updated by Ernest in Mar, 2021

B

Cell Spreading Analysis

Cell spread area | Kymograph generator & analysis

Image location   [Browse]

Save data to   [Browse]

Output settings:
☑ Export data

Image parameters:
Acquisition interval (s):
Pixel size (um):
Smallest cell area (um^2):   (Try 33 um^2)
Image bit depth: 8 / 12 / 16

[Run] [Cancel]

Last updated by Ernest in Mar, 2021

C

Identify spreading cells in the field of view → Perform cell segmentation on individual cells → Measuring cell properties as a function of time
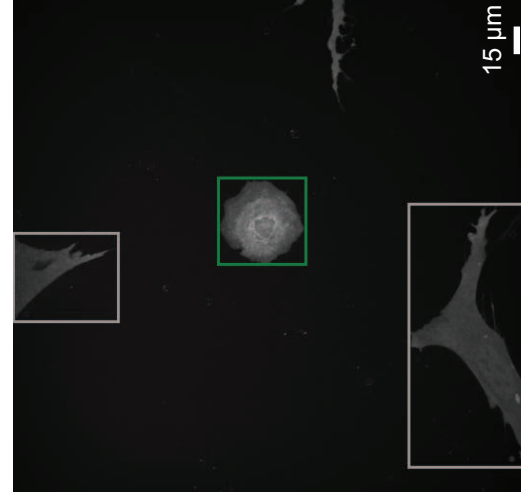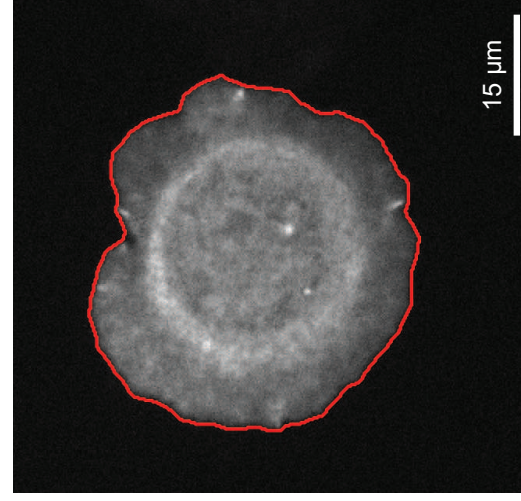
Cell circularity (μm)

Cell spread area (μm^2)

Time (s)

Lag phase | Exponential growth phase | Plateau phase

15 μm

Figure
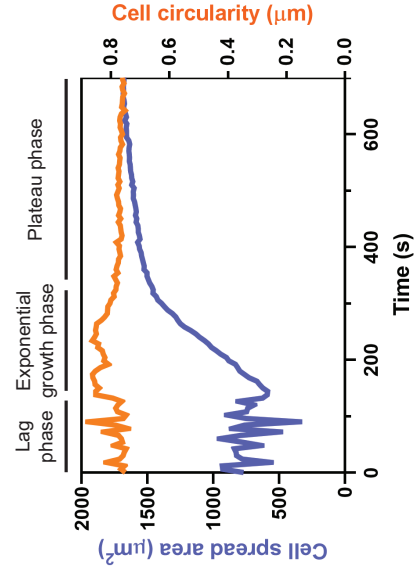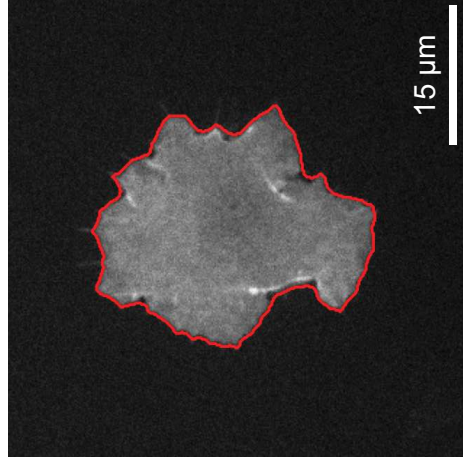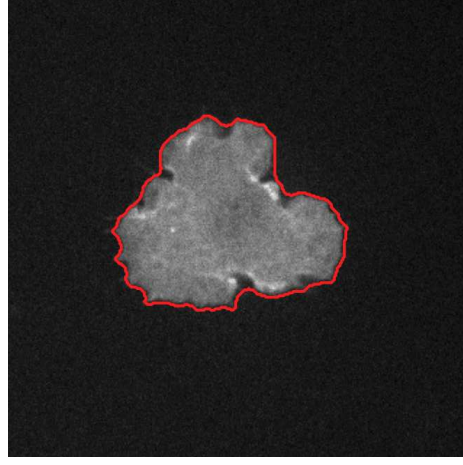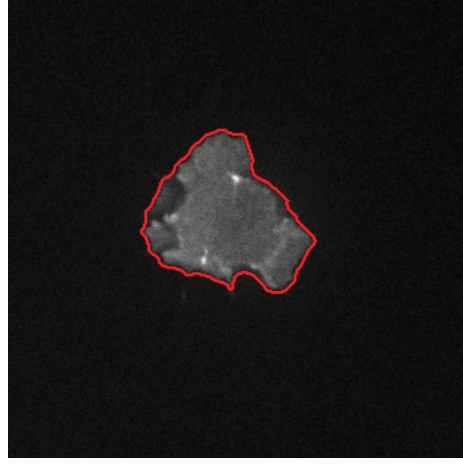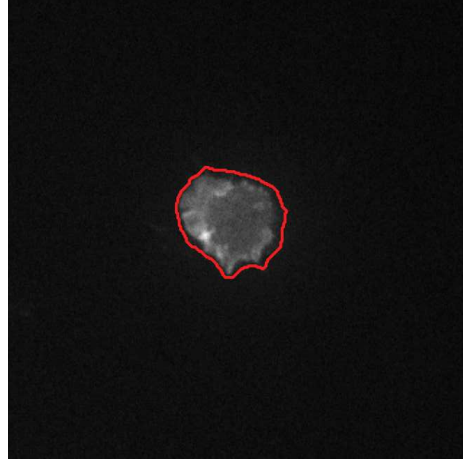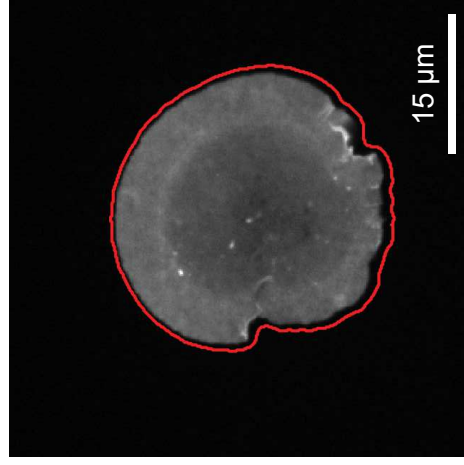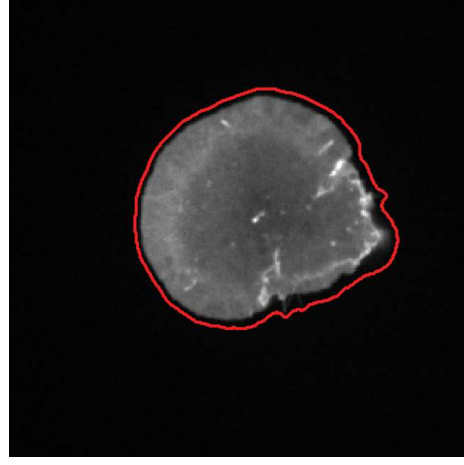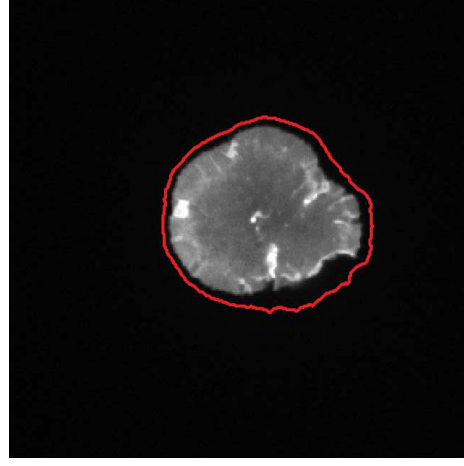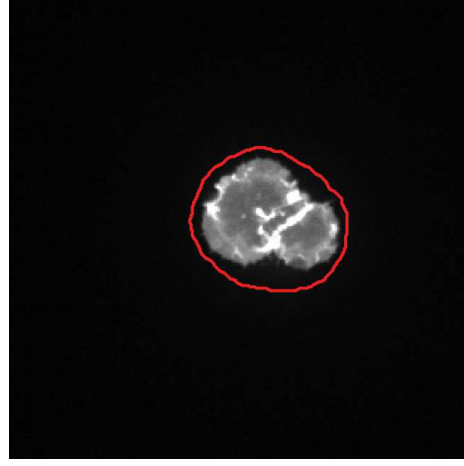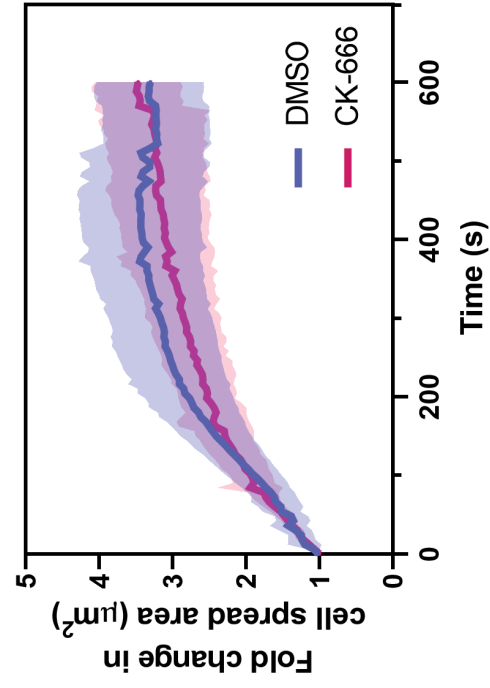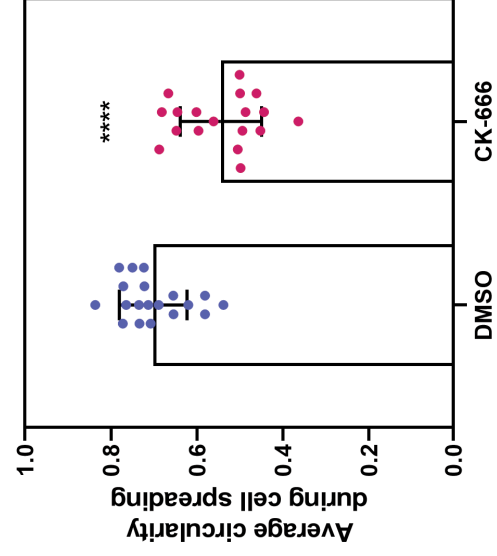
A DMSO

B CK-666

Kymographs
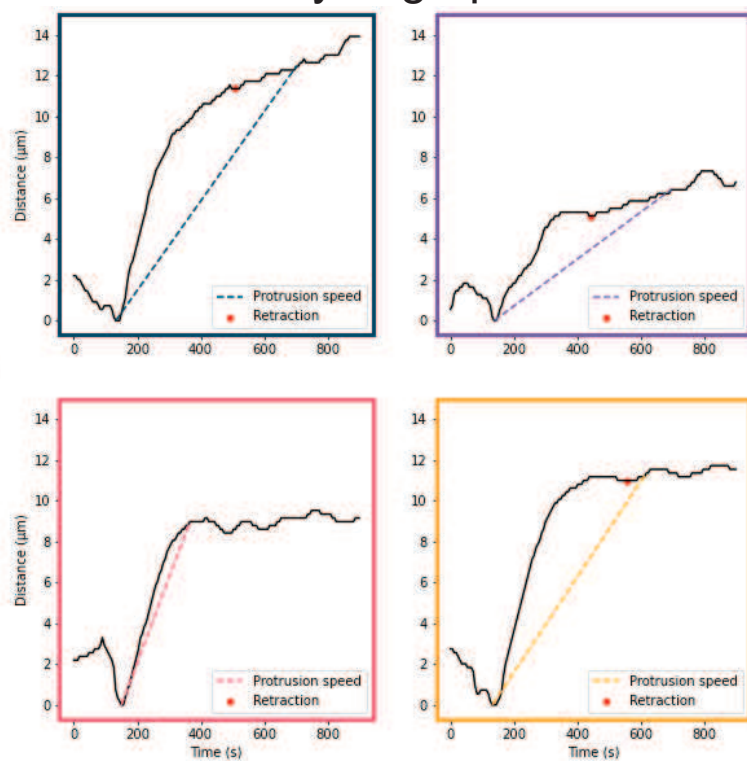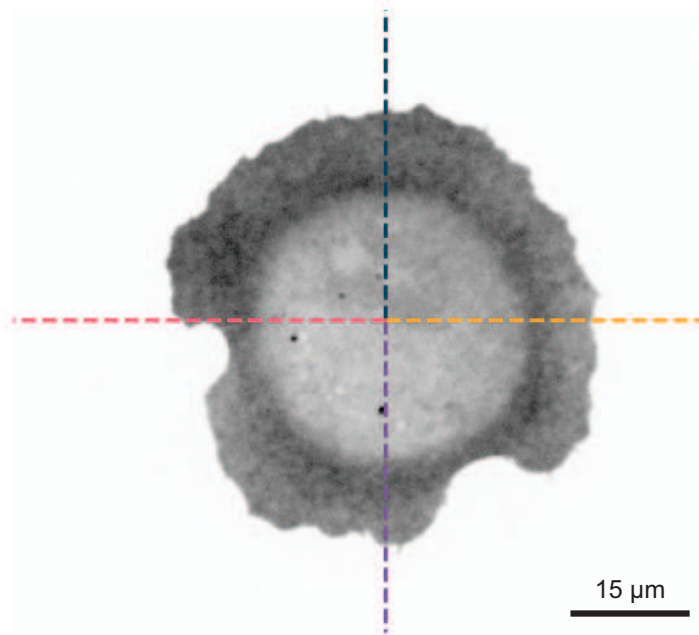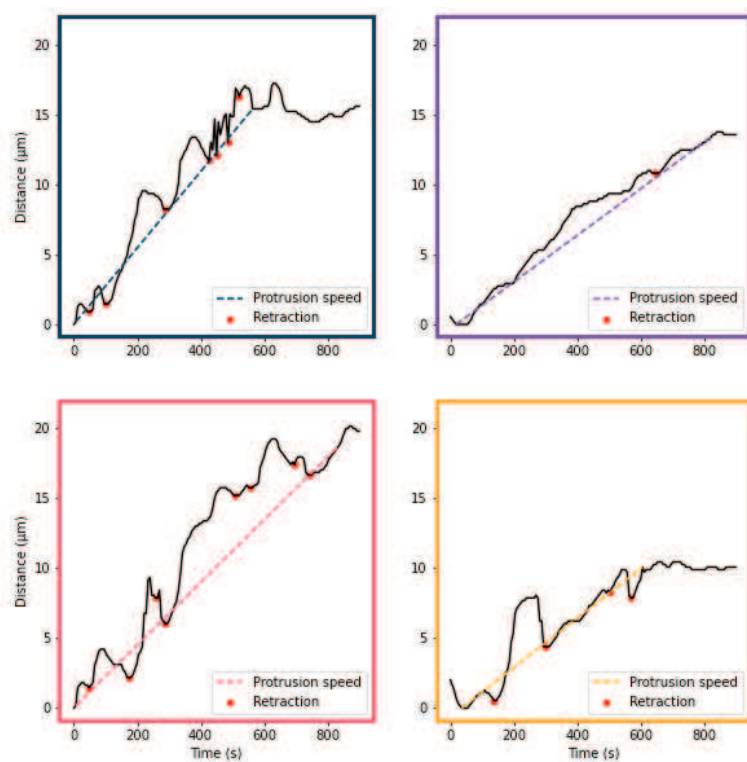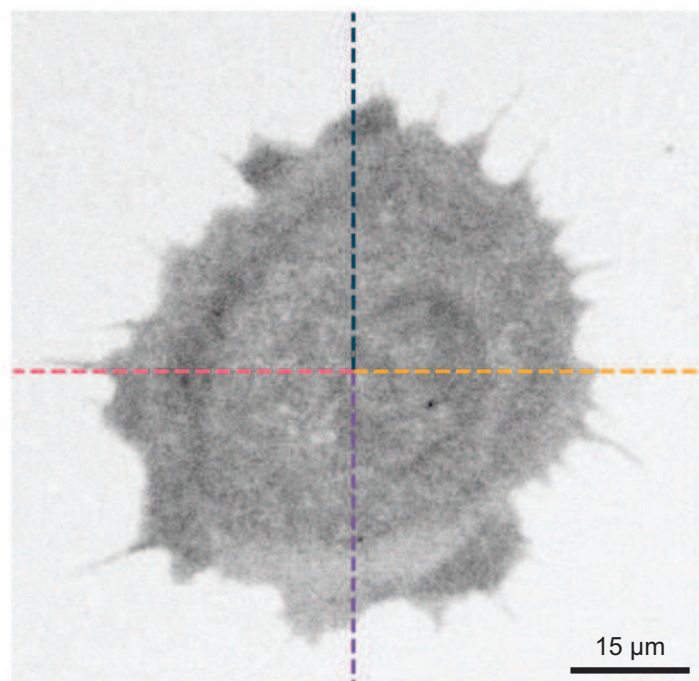
C
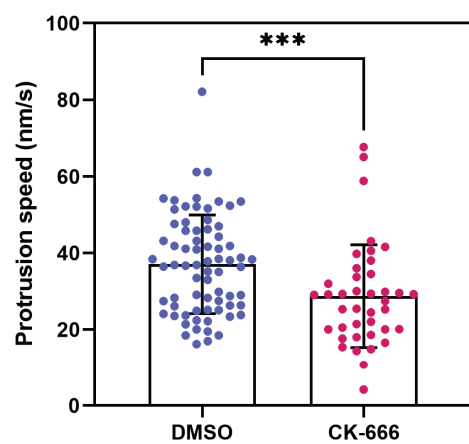
D
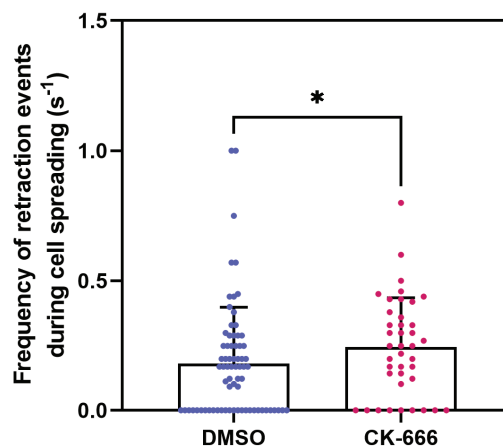
Name of Material/Equipment	Company	Catalog Number	Comments/Description
0.05% Trypsin (0.05%), 0.53 mM EDTA	Wisent Bioproducts	325-042-CL	
10.0 cm Petri Dish, Polystyrene, TC Treated, Vented	Starstedt	83.3902	
15 mL High Clarity PP Centrifuge Tube, Conical Bottom, with Dome Seal Screw Cap, Sterile	Falcon	352097	
1-Well Chamlide CMS for 22 mm x 22 mm Coverslip	Quorum Technologies	CM-S22-1	
35 mm TC-treated Easy-Grip Style Cell Culture Dish	Falcon	353001	
50 mL Centrifuge Tube, Transparent, Plug Seal	Nest	602002	
6.0 cm Cell Culture Dishes Treated for Increased Cell Attachment, Sterile	VWR	10861-658	
Arp2/3 Complex Inhibitor I, CK-666	Millipore Sigma	182515	
Camera, Prime 95B-25MM	Photometrics		
Dimethyl Sulfoxide, Sterile	BioShop	DMS666	
DMEM, 1x, 4.5 g/L Glucose, with L-Glutamine, Sodium Pyruvate and Phenol Red	Wisent Bioproducts	319-005 CL	
DMEM/F-12, HEPES, No Phenol Red	Gibco	11039021	
D-PBS, 1X	Wisent Bioproducts	311-425 CL	
Fetal Bovine Serum	Wisent Bioproducts	080-110	
Fiji Software	ImageJ		

HEPES (1 M)	Gibco	15630080
Human Plasma Fibronectin Purified Protein 1 mg	Millipore Sigma	FC010
Immersion Oil	Cargille	16241
L-Glutamine Solution (200 mM)	Wisent Bioproducts	609-065-EL
MEM Non-Essential Amino Acids Solution (100X)	Gibco	11140050
Micro Cover Glasses, Square, No. 11/2 22 x 22 mm	VWR	CA48366-227-1
Microscope Body, Eclipse Ti2-E	Nikon	
Objective, CFI Plan Apo Lambda 60X Oil	Nikon	MRD01605
Penicillin-Streptomycin	Sigma	P4333
Spinning Disk, Crest Light V2 Spyder	CrestOptics Anaconda	
Stage top incubator	Tokai Hit	
Statistics Software, Prism	GraphPad	
Tweezers, Style 2	Electron Microscopy Sciences	78326-42

Cell & Systems Biology
UNIVERSITY OF TORONTO

March 26th, 2021

Dear Dr Myers,

We are hereby re-submitting our manuscript entitled "Quantitative analysis of cell edge dynamics during cell spreading" (manuscript number: JoVE62369) to JoVE. We appreciate the consideration of the paper and the reviewers' helpful suggestions and insightful criticisms. We are encouraged by the positive comments and have worked hard to address the major concerns in the revised manuscript.

One major issue raised by Reviewer #2 is regarding the quantification of protrusion speed in the kymograph analysis section. In the previous manuscript, we quantified protrusion speeds of the spreading cells by taking the slope between the first local minimum and the last data point, which means that the length of the image acquisition would affect the measurement of the protrusion speed. To overcome this problem, we incorporated a curve-fitting function in our analysis such that we can now derive the plateau phase of the protrusion, which is used to compute the average protrusion speed. With this new implementation, we found a statistical difference in the protrusion speeds of control and Arp2/3-inhibited cells.

Another major issue raised by all 3 reviewers concerns the recovery step after trypsinization. Reviewers questioned the necessity of the recovery step and the method by which we identified the duration of the recovery. We regret having not addressed these questions in the previous manuscript. In the revised manuscript, we added a figure (Figure 2) that demonstrates how the length of the recovery step changes the rate and variability in cell spreading speed. We found that cells recovering for 45 mins exhibited faster and more synchronized cell spreading than cells which were allowed to recover for shorter periods of time.

To address reviewers' suggestions, we have refined the manuscript so that it now reflects live cell spreading assays present in the literature, contains fewer over-generalized statements, and presents a more fluid, less cluttered protocol.

We are immensely grateful for the reviewers and their comments, and we hope that our responses summarized in the following pages alleviate the concerns and make the manuscript acceptable for publication in JoVE.

Sincerely,

Sergey V Plotnikov, PhD
Assistant Professor
Department of Cell & Systems Biology
University of Toronto

Reviewer comments:

Reviewer #1:

1. *"Others have used live cell spreading assays for years (MP Sheetz). It would be good to mention these and not just those endpoint assays that examine fixed cells in the introduction."*

   We are aware of a large body of papers on cell spreading and lamellipodia dynamics published by the Sheetz lab and we apologize for not citing a few of these papers in the manuscript. As the reviewer suggested, we expanded and revised the introduction to acknowledge the contribution of the Sheetz group. We also briefly described the advantages and limitations of the protocols described in those papers. The following text was added (page 2):

   "To determine the molecular mechanisms that control lamellipodia dynamics, the Sheetz group pioneered the use of quantitative analysis of live spreading cells and uncovered many fundamental properties of cell edge protrusions[11, 12, 22]. These studies have demonstrated that the live-cell spreading assay is a robust and powerful technique in the toolbox of a cell biology laboratory. Despite that, a detailed protocol and open-source computational tool for a live-cell spreading assay are currently unavailable for the cell biology community."

2. *"What are the advantages and disadvantages of this approach vs. manual or in house analysis approaches used in the past."*

   We apologize for the vague description of the advantages and disadvantages of automated segmentation. We added the following text to the discussion section (page 15):

   "Our image processing and analysis software performs a streamlined analysis of the spreading cells, from cell segmentation to data quantification. Manual image analyses of cell spreading usually involve biased selection of a threshold value or applying an automated segmentation algorithm, which is not suited for high-throughput experiments where many images need to be analyzed. Our software is, therefore, designed to detect and segment spreading cells in an automatic fashion, in addition to quantifying protrusion dynamics and morphological descriptors. Together, these features make the described protocol amenable for large-throughput screenings of signaling pathways and molecular players that regulate lamellipodia."

3. *"The introduction reads like the innovation is live cell protrusion assays, but isn't the innovation the specific analysis approach?"*

   We agree with the reviewer that the novelty of spreading assay was overstated in the initial submission. We modified the introduction as follows (page 2):

   "These studies have demonstrated that the live-cell spreading assay is a robust and powerful technique in the toolbox of a cell biology laboratory. Despite that, a detailed protocol and open-source computational tool for a live-cell spreading assay are currently unavailable for the cell biology community. To this end, our protocol outlines the procedures of imaging live spreading cells and provides an automated image analysis tool."

4. *"Abstract: ...the cell spreading assay or ... cell spreading assays." And "There was an instance of using trypsin-EGTA instead of trypsin-EDTA. Was that intentional?"*

We apologize for the typos in the manuscript. All typos were corrected in the revised manuscript.

5. *"Perhaps both trypsin and not proteolytic cell adhesion blockers could be mentioned as there is less chance for integrin cleavage. Is there much difference between allowing cells to "rest" before spreading and using non-proteolytic approaches for detaching cells?"*

We are very grateful to the reviewer for this suggestion. We did not mention proteolytic cell adhesion blockers in the original submission because this cell detachment technique is rarely used for strongly adherent fibroblasts. However, we agree that non-proteolytic cell detachment might be a good alternative to trypsin for the readers working with weakly-adherent cells. Thus, the revised protocol contains a note suggesting non-proteolytic cell detachment for weakly adherent cell. The following note was added to page 5 under Step 2.6:

"**NOTE:** If applicable, trypsin can be replaced by a non-proteolytic cell adhesion blocker."

*We included an additional figure to demonstrate the importance of the recovery period for the analysis of cell spreading **(Figure 2)**. We plated cells recovered for 0 to 45 minutes on fibronectin-coated coverslips and let them to spread for 15 minutes. Then we fixed the cells and analyze the distribution of the cell area. We found that cells recovered for longer time (up to 45 mins) exhibited dramatically lower cell-to-cell variability in cell area compared to their counterparts that did not recover after trypsinization or recovered for a short period of time. The following text was added to the Results section to describe these data (pages 11):*

"During the recovery step, cells replenished their integrin receptors on the plasma membrane as indicated by the fast and synchronous attachment of the recovered cells to the fibronectin coated coverslips **(Figure 2)**. Without the recovery, cells spread for 15 minutes exhibited a broad distribution of cell size indicating a high variability in the onset of cell spreading **(Figure 2A and B)**."

Reviewer #2:

1. *"However, the major scientific issue that I have is in the "protrusion speed" measurement. The authors are taking the lowest point in the kymograph in the first half of the movie and going to the terminal time point. Therefore, the length of the imaging is critical in determining their "protrusion speed", and their protrusion speed includes retractions. This is very difficult to avoid. But as you can see in Figure 4, some cells have a steady spreading rate that plateaus, and some cells edges appear to still be spreading at the end of the imaging, especially the CK666 cell. I wonder if some tweaking or addition here would more accurately measure aspects of protrusion?"*

We thank the reviewer for pointing out this fundamental flaw in our analysis. To address this concern, we implemented a curve fitting module that detects the rapid expansion and the plateau phases of the protrusion and excludes the latter phase when computing the average

*protrusion speed (**Supplemental Figure 1**). Using this modified analysis, we revealed a statistically significant difference in the cell protrusion speed between control and CK-666 treated cells. Therefore, we modified the Results section as follows (page 13):*

"The analysis of cell edge speed revealed a moderate but significant decrease in the average protrusion speed of Arp2/3-inhibited cells compared to control (Control: 37.1 ± 12.87 nm/s vs. CK-666: 28.7 ± 13.4 nm/s, p = 0. 9 x 10^{-3}) **(Figure 5C)**."

2. *"Line 89: The authors are using PH-Akt-GFP. They might inform the reader why they are using this probe, and what other reporters would also be suitable. Would a diffuse fluorophore work or do we need cortical or membrane fluorophore? Perhaps a number of Addgene #s to guide the user to some appropriate examples would also be useful."*

We agree with the reviewer that membrane targeted fluorophore is not required for the described assay. Soluble GFP or any other fluorescent marker evenly distributed in the cytoplasm will work as well as PH-Akt-GFP. Our rationale to perform these experiments on MEFs with genetically integrated PH-Akt-GFP was (i) homogeneous cell population with similar expression of the fluorescent marker in every cell, and (ii) even distribution of the fluorophore in the cytoplasm with barely noticeable enrichment at the protruding cell edge. In preliminary experiments, we also tested fluorescent markers localized on the plasma membrane. We found the fluorescent proteins (eGFP and mCherry) tagged with CAAX domain tend to aggregate in the cytoplasm or retain in the membrane compartments, creating extremely bright spots in the perinuclear area of cells. Since our segmentation algorithm is optimized for images with bimodal distribution of pixel intensities (i.e. background and foreground pixels), such bright spots creating another mode on the intensity histogram decrease the accuracy of cell segmentation. Thus, we do not recommend using CAAX-eGFP and CAAX-mCherry in the cell spreading assay. The following note was included in the Protocol section to address this reviewer's concern (page 3):

"**NOTE:** The described cell spreading protocol was performed using mouse embryonic fibroblasts (MEFs) expressing PH-Akt-GFP (a fluorescent marker for PIP_3/$PI(3,4)P_2$). This cell line was generated by genomically integrating an expression construct for PH-Akt-GFP (Addgene #21218) by CRISPR-mediated gene editing. However, other fluorescent markers that are expressed transiently or integrated in the genome can also be used in this assay. For optimal image segmentation, we recommend using fluorescent markers that are evenly distributed in the cytoplasm, *e.g.,* cytosolic GFP."

3. *"Can the authors provide a sample data set? I think many users would find this useful to get started. I would also like to test out the code on my system."*

We greatly appreciate reviewer's interest in our software and the suggestion to provide a sample dataset. It is a great idea that we did not think about! We added two sample datasets to a publicly accessible cloud storage at: https://www.dropbox.com/sh/dik21h1fnbaqhlg/AAB314RZT7AF6o6mLadLimYaa?dl=0. We provide link to the sample dataset in the README file in the Github repository.

4. *"Line 113 section 1.9: When we want individual cells plated without clumping we filter them through a 100 um filter, commonly used in FACS facilities. This might be helpful for some readers."*

As the Reviewer suggested, we added the following to the Protocol section (page 3):

Step 1.8: "Pipette 1 mL of the trypsinized cells into the 15 mL centrifuge tube in order to dilute the cells. Pipette the contents of the tube up and down to ensure an even distribution of cells within the media. For cell types with high aggregation propensity, filtering cells through a cell strainer (100 μm mesh size) is recommended to minimize the occurrence of cell clumping."

5. *"Line 219 section 4.2: Is it possible to state what resolution might be the minimum to enable the kymographs? This might help orient some readers that want to use lower NA air objectives for high throughput."*

We tested movies with different pixel size generated by binning our existing images and resolved protrusions and quantified their dynamics even when the pixel size was as large as 0.5mm. So, we believe that 20x objective would be sufficient for the cell spreading assay and should definitely be considered for high-throughput experiments. However, since most low magnification objectives have relatively low numerical aperture, such objective might be unable to provide desired image quality (signal-to-noise ratio) and/or result in excessive photobleaching of the cells. In our experiments, 60X/1.4NA objective combined with the large field of view spinning disk scanner (Crest V2) and 25mm sCMOS camera (Prime 95b) was an optimal choice allowing us to image 2-4 spreading cells per field of view with high frame rate and moderate photobleaching. We modified the protocol to reflect these considerations (page 6):

"**NOTE**: We use a 60X, 1.4 N.A. oil immersion objective in this protocol because of its reasonably large field of view and outstanding light collection efficiency. If a larger field of view is required, a lower magnification objective can be used as long as the signal-to-noise ratio of the images is greater than 2.5.

6. *"Line 242 section 4.8: How did the authors come to the 6 second sampling frequency? In my experience, most cells are going to have a different spreading rate. I think instead of specifying here, the authors might guide the readers what they might do to determine the optimal sampling frequency, and advise them that the authors use 6 seconds as the starting point. For example, if someone wanted to use this protocol for immune cells spreading on activated coverslips, they'll need to image much faster I think. Those cells are crazy fast spreaders. Stupid fast. Crazy."*

We thank the reviewer for this suggestion. We agree that different cell types exhibit very different spreading speed, and this point should be addressed in the protocol. Therefore, we added the following note to section 4.7 of the Protocol (page 6 - 7):

"**NOTE:** Due to the high variability of lamellipodia protrusion velocity among different cell types, the optimal frame rate should be determined empirically. The imaging interval of 6 seconds used in our experiments is a good starting point for the analysis of many

mesenchymal and epithelial cells. However, cells that spread very quickly (*e.g.*, immune cells) may require a much higher frame rate (shorter imaging interval). The optimal frame rate for cell spreading movies ensures a 2-5 pixels displacement of the protruding cell edge between subsequent frames. Considering the accuracy of curve fitting used to identify the plateau of cell spreading, the optimal frame rate should also ensure 50-100 measurements of cell edge displacement during the rapid expansion phase of cell spreading. The number of fields of view should be adjusted depending on the exposure time, the distance between acquisition points, and the stage movement speed. Users are advised to determine the maximum number of fields of view that can acquired with the desired frame rate."

7. *"Line 263 section 5.1: I think stating what the goal here is would help users expedite the process. "Images need to be in tiff format and the pixel size in microns is needed. You can export your images from your acquisition software as tiff or use the following steps in FIJI. If your files are already in tiff format then skip to step XX.*

   As the reviewer suggested, we added the following text to the protocol to help users expedite the process (page 7):

   "**NOTE:** The software requires an image in .tiff format and a pixel size as the input parameters. Both requirements can be fulfilled using the acquisition software or Fiji (in this protocol). If these requirements are fulfilled, proceed to step 5.2."

8. *"Is there a reason the functions can't be in a single python file? The GUI build is great. However, there seems to be some points where the authors might want to change components in the code but not built into the GUI. Perhaps the authors could look through and make sure these points are carefully annotated for what they might change and why?"*
   The python script we developed is modular, composed of the GUI, the segmentation algorithm, the data analysis module etc. In our opinion, such structure of the script makes any further edits and modifications easier, so we would like to keep it. We apologize for not including annotations (or comments) in the initial submission. We provide the revised scripts with docstrings and comments as supplemental files for this manuscript. We also uploaded these files to the Github repository.

Reviewer #3:

1. *"In the intro and throughout the manuscript, the authors seem to make the point that lamellipodia are essential for cell spreading or constitute the structural organelle to mediate specific spreading. This is actually a misleading statement and thus cannot stand as the authors put it at present! Indeed, the authors themselves show that inhibition by CK666 of Arp2/3 complex (which is considered to be essential for the protrusion of lamellipodia) has only very modest effects on spreading efficiency, at least if considering these very short time points (up to 15 minutes), which the authors claim are the only relevant ones for spreading. The authors also fail to refer in this context to a study they are even citing (ref 10), in which it is shown very clearly that cells lacking lamellipodia (due to genetic removal of Rac1 GTPase) can still spread efficiently. I see the authors' point that the latter study looked at spreading with much longer time points (and thus may have missed*

subtle differences up to the 15 minute-time point, for instance). However, spreading was by no means completed in these conditions and cell type after 15 minutes in the experiments described in ref 10, and thus the data used in the present and aforementioned study cannot be directly compared! Indeed, most studies published on spreading efficiency so far look at much longer time periods than the authors here, so to claim that everything is finished (plateauing by 15 minutes), is certainly misleading and too generalized."

We apologize for the confusion about the role of lamellipodia in cell spreading. We certainly do not think lamellipodia are required for cell spreading, nor cell migration and we agree with the reviewer that the correct interpretation of cell spreading assay results might (and often does) require additional experiments, such as immunostaining for known lamellipodia and filopodia markers. However, description of these techniques and experimental design for studying lamellipodia dynamics is certainly outside the scope of this protocol.

We are aware that many published protocols of cell spreading assay were performed on a much longer timescale. The timescale of cell spreading assay described here was determined empirically but is also supported by a large body of published studies. Cai et al., 2006 have showed previously that the average time for MEF cells to reach to their fully spread stage on fibronectin is ~16 min. Similarly, in our hands, MEFs reached a plateau phase within first 15 mins of cell spreading. Several other studies published by the Sheetz group (Dubin-Thaler.Sheetz.2008., Wolfenson.Sheetz.2014) have also reported that isotropic expansion of spreading cells detected by a rapid (≈5mm/min) protrusion of the cell edge occurs within the first 15 minutes after plating. Following this rapid expansion, cells polarize and downregulate their protrusive activity. The decrease in protrusion speed during the late stages of cell spreading was previously attributed to an increase in membrane tension (Raucher.Sheetz.2000, Gauthier.Sheetz.2011, Wolfenson.Sheetz.2014). Since membrane tension is an important, but indirect, regulator of actin dynamic at the cell leading edge and lamellipodia protrusions, we restricted our analysis by the first 15 min of cell spreading when the endogenous activity of actin polymerization machinery is mostly unaffected by external factors.

2. *"In the intro (lines 59/60), the authors word that "Compared to the highly variable lamellipodia of migrating cells, the lamellipodia of spreading cells are much more uniform and stereotypical..." This will definitely depend on cell type and conditions, so overgeneralized statements of this kind should be omitted (think of the efficiently migrating keratocytes using highly uniform lamellipodia or hemocytes in Drosohila perhaps, so oversimplified statements of this kind are certainly not helpful)."*

We agree with the reviewer that the morphology and dynamics of protruding cell edge vary greatly among different cell types. But we would argue that fish keratocytes and Drosophila hemocytes are rather rare exceptions in the multitude of cell types with highly variable lamellipodia. We are certain that for a generic mammalian cell variability of lamellipodia protrusions is much higher for migrating rather than for spreading cells.

3. *"The authors also make a huge point about trypsin sort of digesting off extracellular portions of transmembrane proteins, such as integrins, for instance, and thus recommend to force cells to stay in suspension for a quite long period of time (at least 45 minutes as far*

as I understand) before seeding. The authors should be informed that such a treatment is not useful for various cell types, and might lead to exaggerated cell-to-cell sticking etc, so cannot be recommended as general rule for spreading assays in all cell types and conditions! I do admit, though, that it is possible that the rapid plateau in cell spreading (after roughly 15 minutes) observed by the authors here might derive from the fact that keeping the cells in suspension before seeding allows them to recover perhaps from potential adverse effects of trypsin. However, this is sole speculation at present, and if this is a realistic possibility, it should be discussed and experimentally tested in fact! In other words, it would be much more convincing if the authors actually tested whether the plateau is reached later if this forced time in suspension is omitted."

We appreciate the reviewer's concern for the necessity of the recovery step after trypsinization. Also, we are aware that a prolong maintenance of cells in suspension is deadly for non-transformed adherent cells. To address this concern and inform users on the biological effects of cell of this consideration, we included the following (page 4):

"**NOTE:** The duration of recovery time may vary for different cell types. Although in our experiments 45-minute-long recovery had a negligible effect on cell viability, some cell types may undergo anoikis when maintained in suspension for too long. Therefore, we recommend determining the optimal recovery time empirically. The optimal recovery time enables fast and synchronous cell spreading with no dead or apoptotic cells in the sample."

*Furthermore, we included an additional figure to demonstrate the importance of the recovery period for the analysis of cell spreading (**Figure 2**). We plated cells recovered for 0 to 45 minutes on fibronectin-coated coverslips and let them to spread for 15 minutes. Then we fixed the cells and analyze the distribution of the cell area. We found that cells recovered for longer time (up to 45 mins) exhibited dramatically lower cell-to-cell variability in cell area compared to their counterparts that did not recover after trypsinization or recovered for a short period of time. The following text was added to the Results section to describe these data (pages 11-12):*

"During the recovery step, cells replenished their integrin receptors on the plasma membrane as indicated by the fast and synchronous attachment of the recovered cells to the fibronectin coated coverslips **(Figure 2)**. Without the recovery, cells spread for 15 minutes exhibited a broad distribution of cell size indicating a high variability in the onset of cell spreading **(Figure 2A and B)**."

Finally, we added a note suggesting non-proteolytic cell detachment for the readers working with weakly-adherent cells. Thus, the revised protocol contains a note suggesting non-proteolytic cell detachment for weakly adherent cell. The following note was added to page 5 under Step 2.6:

"**NOTE:** If applicable, trypsin can be replaced by a non-proteolytic cell adhesion blocker."

4. *"The authors employ a 60x oil immersion objective, and propose to select 4 independent cells (fields of viee, meaning very low throughput) for filming cells during the spreading process. Indeed, using an oil immersion objective is limiting the field of view to a very small*

area on the coverslip, as the oil will not easily spread over long distances on the bottom coverslip surface. So I wonder why the authors don't use high NA air objectives, which may lead to much better results, although the reason perhaps includes the fact that air objectives are usually much less light-sensitive, and may thus be of limited use for fluorescence as used here. This then actually brings me back to the point that the necessity of the method to require fluorescence is actually a real limitation here - aside from the points already mentioned in this context above."

We tested movies with different pixel size generated by binning our existing images and resolved protrusions and quantified their dynamics even when the pixel size was as large as 0.5mm. So, we believe that 20x objective would be sufficient for the cell spreading assay and should definitely be considered for high-throughput experiments. However, since most low magnification objectives have relatively low numerical aperture, such objective might be unable to provide desired image quality (signal-to-noise ratio) and/or result in excessive photobleaching of the cells. In our experiments, 60X/1.4NA objective combined with the large field of view spinning disk scanner (Crest V2) and 25mm sCMOS camera (Prime 95b) was an optimal choice allowing us to image 2-4 spreading cells per field of view with high frame rate and moderate photobleaching. We modified the protocol to reflect these considerations (page 6):

"**NOTE**: We use a 60X, 1.4 N.A. oil immersion objective in this protocol because of its reasonably large field of view and outstanding light collection efficiency. If a larger field of view is required, a lower magnification objective (*e.g.*, 20x) can be used as long as the signal-to-noise ratio of the images is greater than 2.5."

5. *"In the discussion (line 563), the authors state that the employed "…image processing routine reduces bias in data analysis", which is certainly not justified, because I wonder why and in which way would there be less bias using this method as compared to simply fixing cells at given time points and staining them to assess spreading efficiency...? Such misleading statements should definitely be avoided, as they will confuse the reader!"*

We apologize for such an ambiguous statement. We clearly have no data to prove such statement. Therefore, we modified the discussion in page 15 as follows:

"Our image processing and analysis software allows for a streamlined analysis of the spreading cells, from cell segmentation to data quantification. Manual image analyses of spreading cells often involve manually determining a global threshold value or applying an automated segmentation algorithm in an image analysis software, such as ImageJ, and then measure different aspects of cell spreading. While such manual workflow is applicable to low throughput experiments, it is not suited to higher throughput experiments where a large number of images need to be analyzed. Our software is, therefore, designed to detect and segment spreading cells automatedly and to quantify the morphological descriptors and protrusion dynamics. Together, these features make the described protocol amenable for large-throughput screenings of signaling pathways and molecular players that regulate lamellipodia.*"

6. *"In lines 610/611 of the discussion, the authors state that "...it is also important to highlight that this live cell spreading protocol is a robust and powerful tool to study the dynamics of lamellipodia". Again, this statement is entirely misleading if assuming that spreading can also occur efficiently in the absence of lamellipodia. In other words, the authors must consider that lamellipodium protrusion and cell spreading can definitely be functionally separated, as shown by others in the field previously. So in conclusion, spreading certainly constitutes an interesting parameter to look at, but if readers would like to study lamellipodia dynamics, they should be advised to study cells and conditions forming lamellipodia in a robust and reproducible fashion, and not just spreading, which may or may not involve lamellipodium protrusion!"*

We agree with the reviewer that lamellipodial protrusion and cell spreading can be functionally separated as seen in our experimental data. However, we don't think that these data prevent us from using cell spreading as a simple model to study lamellipodia protrusion. as long as we understand the limitations of this assay. In fact, a substantial body of published work have shown that lamellipodia formed during migration and cell spreading are structurally identical (Gauthier.Sheetz.2011, Wolfenson.Sheetz.2014, Cai.Sheetz.2006, Giannone.Sheetz.2004, Raucher.Sheetz.2000). These lamellipodia also consist of the same molecular species (e.g., actin, focal adhesion components, myosin, etc.) and exhibit very similar pattern of protrusive activity.

$$y = \frac{c}{1 + ae^{(-bx)}}$$

Logistic model

Experimental data

Frame

Distance (pixel)
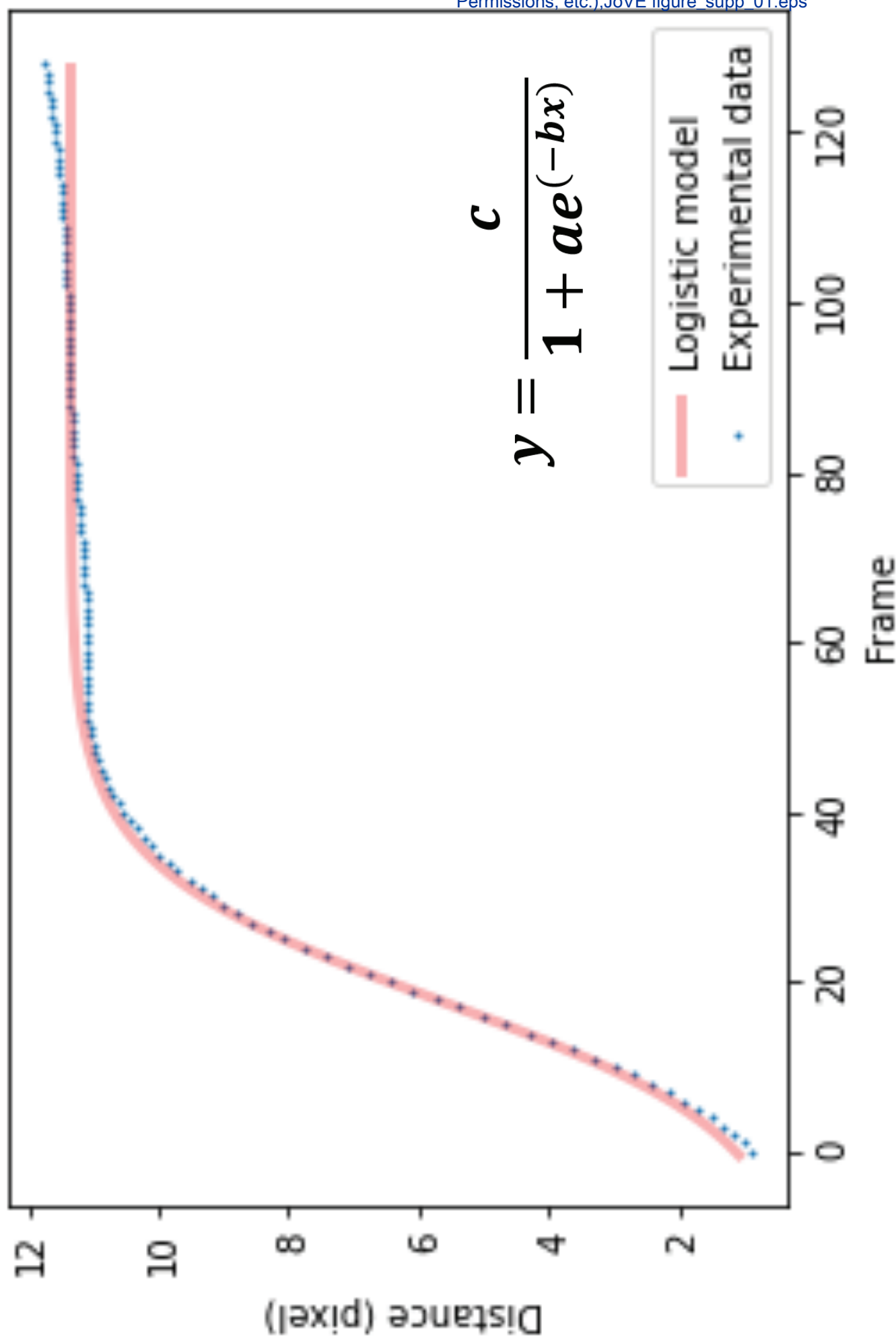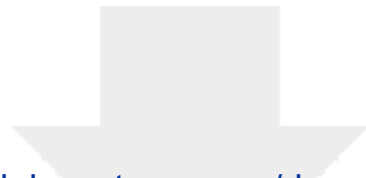
cell_segmentation_no_crop
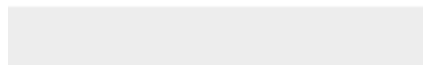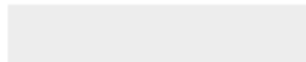
Click here to access/download

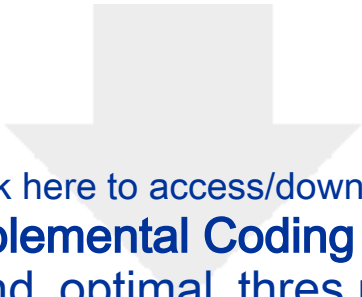**Supplemental Coding Files**

cell_spreading_gui_version.py

Click here to access/download
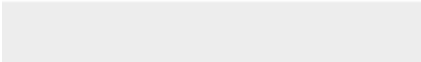**Supplemental Coding Files**
cell_spreading_GUI.py

Click here to access/download
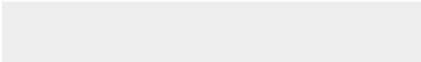**Supplemental Coding Files**
crop_cell_function.py

Click here to access/download
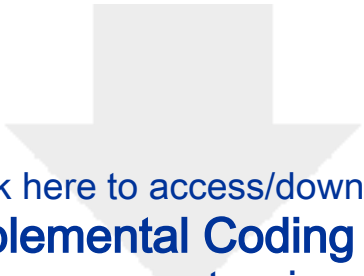
Supplemental Coding Files
find_optimal_thres.py

Click here to access/download
Supplemental Coding Files
find_relevant_max.py

Click here to access/download

Supplemental Coding Files

kymographs_generator_gui_version.py